POLITECNICO DI BARI

DIPARTIMENTO DI INGEGNERIA ELETTRICA E DELL'INFORMAZIONE (DEI)
MASTER'S DEGREE IN AUTOMATION ENGINEERING

APPLIED MECHANICS – FUNCTIONAL DESIGN

Gear Gripper with parallelogram mechanism

Design, Motion Analysis and Simulations

Professor:

Prof. Eng. Mario Massimo Foglia

Students:

Savino Francesco

Savino Tommaso

Academic Year 2022/2023

Table of contents

List of figures

Abstract

This project focuses on the design, kinematic study, static study and simulation of a gripper with a parallelogram mechanism, realised using SolidWorks.

The main objective was to create a device capable of gripping objects while maintaining a constant orientation due to the configuration of the parallelogram mechanism. The design phase included modelling the gripper and defining the critical parameters for optimal operation.

Subsequently, kinematic simulations were performed to analyse the behaviour of the gripper. The results demonstrate the mechanism's effectiveness in ensuring a stable and precise grip.

Introduction

The project described in this report concerns the design, kinematic study and simulation of a gripper with a parallelogram mechanism, using SolidWorks. The methodological approach adopted was structured in several stages, each of which contributed significantly to the realisation of the project.

Initially, a preliminary study was conducted based on transformation matrices according to the Denavit-Hartenberg convention. This method made it possible to systematically describe the geometry of the parallelogram mechanism. This analysis provided a solid theoretical basis for understanding the kinematic behaviour of the system.

After completing the theoretical studies, we moved on to the modelling and design phase in SolidWorks. In this phase, individual parts of the gripper were created and subsequently assembled into a complete model.

Once the gripper assembly was completed, a motion analysis was performed to observe the dynamic behaviour of the mechanism and compare it with what was obtained from the theoretical study. This analysis made it possible to visualise the movements of the gripper fingers and identify any interference problems or limitations in the range of movement.

A further study looked at the variation of torques in relation to the distance between the gripper phalanges and the mass of the object to be gripped.

Finally, gripping simulations were conducted to verify the effectiveness of the design in real scenarios. These simulations tested the gripper's ability to grasp and hold objects of different shapes and weights, confirming the validity of the design. The results obtained demonstrate that the gripper can operate stably and accurately, meeting the initial design requirements and ensuring optimal performance.

1. State of the Art of Robotic Grippers

Robotic grippers are essential components of robotic systems that enable machines to interact with and manipulate objects in a wide range of applications. They function as the "hands" of robots, allowing them to grasp, hold, and release items with precision and control.

Robotic grippers are available in various designs, each tailored to specific tasks and requirements.

They are of crucial importance in several industrial sectors, including manufacturing, logistics, healthcare, and agriculture. The use of automation and robotic systems in these sectors has the potential to enhance efficiency, productivity, and safety.

The primary function of robotic grippers is to securely grasp objects of different shapes, sizes, and materials. These can be classified into several categories based on their design, mechanism, and functionality.

Research was conducted on the current types of grippers available in the market. The grippers can be classified according to the gripping method:

1. **Pressure gripper** (*parallel gripper*): This type of gripper is used for pieces that can be pressed by the gripper without deformation. There are two fingers moving in parallel.

Figure 1: Pressure gripper

2. **Coupling gripper**: This kind of gripper is utilized for large-sized pieces that cannot be pressed by the gripper.

Figure 2: Coupling gripper

3. **Vacuum gripper**: Vacuum grippers are employed in robots for grasping non-ferrous objects. They utilize vacuum cups as the gripping mechanism, commonly known as suction cups. This type of gripper provides effective handling for smooth, flat, and clean objects, featuring only one surface for gripping. Importantly, it is not ideally suited for handling objects with pores.

Figure 3: Vacuum gripper

4. **Electromagnetic gripper**: magnetic grippers are typically utilized in robots as end effectors for gripping ferrous materials.

Figure 4: Electromagnetic gripper

5. **Needle gripper**: these grippers utilise thin needle-shaped probes to penetrate and grip objects. They are suitable for objects with small holes or limited gripping surfaces.

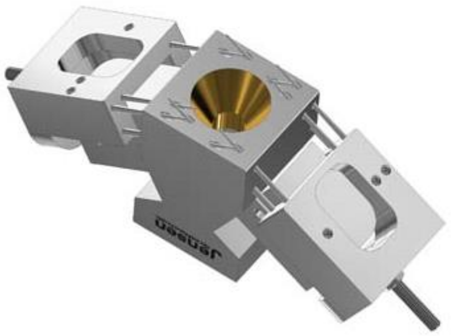

Figure 5: Needle gripper

Another common classification is that based on the *number of fingers*:

1. **Two-fingers grippers**: these grippers are equipped with two fingers or claws that facilitate the grasping and manipulation of objects. They are straightforward, cost-effective, and well-suited to numerous industrial applications.

Figure 6: Two-fingers grippers

2. **Three-finger grippers**: are designed for users requiring more advanced grasping and manipulation capabilities. They are more precise and accurate, which makes them suitable for handling delicate and fragile objects.

Figure 7: Three-finger grippers

Grippers can also be classified according to actuation:

1. **Pneumatic grippers**: these are actuated by compressed air or gases and provide fast and powerful gripping capabilities.
2. **Electric grippers**: they use electromechanical motors or actuators to grip and release objects.

Or based on specialized *applications*:

1. **Soft grippers**: are constructed from flexible materials such as elastomers or soft robotics components. They are capable of conforming to a variety of object shapes and are suitable for handling delicate or irregularly shaped objects.

Figure 8: Soft grippers

2. **Adaptive grippers**: are designed to adjust their finger positions or shapes to accommodate objects of different sizes, shapes, or textures.

Figure 9: Adaptive grippers

Two distinct *gripping techniques* exist:

1. **Force-lock grip**: the object is supported only by frictional forces between the surface of the object and the gripping fingers. This technique necessitates the use of jaws made of materials with a high coefficient of friction in relation to the material of the object to be gripped.
2. **Shape-lock grip**: this is achieved through the adaptation of jaws to the shape of the object, which allows for the distribution of force along the contact surface. The support is generated almost exclusively by the restraint of the object, resulting in a lower force requirement for gripping than with a corresponding force lock gripper.

In addition to the gripping method and technique, it is also important to classify the *type of contact* to be made between the gripper and the object to be manipulated. The active areas may vary depending on the method employed. The following are the four main categories of contact:

(a) Contact at a point

(b) Contact along one line

(c) Contact along two lines

(d) Contact on a surface

The study [1] highlights the various types of grippers contact in relation to the object to be gripped:

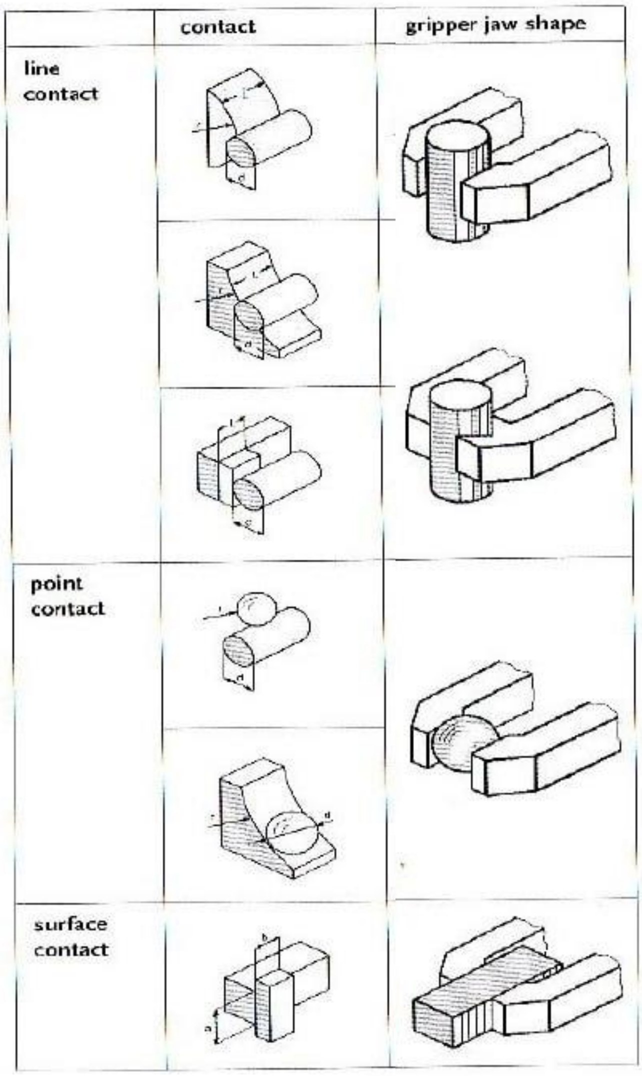

Figure 10: Various types of grippers contact in relation to the object to be gripped

Two types of grippers can be distinguished based on their *movement*:

1. **Rotation Movement**: As evident in the image [x], the gripper relies on rotational movement to grasp objects.

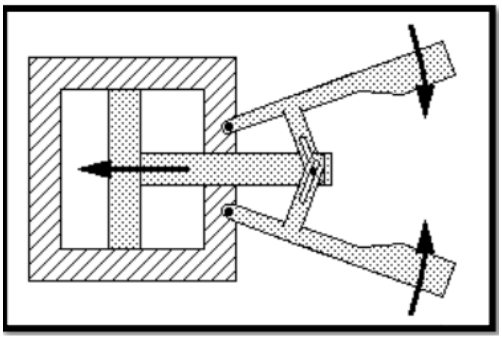

Figure 11: Example of gripper with rotation movement

2. **Translation Movement**: As depicted in the picture [x], the gripper operates using a translational movement to grasp objects.

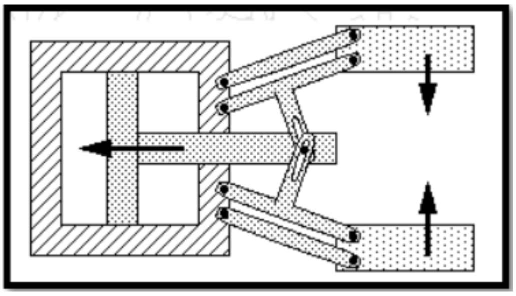

Figure 12: Example of gripper with translation movement

Since it was chosen to design a pressure gripper with a translational movement, numerous design possibilities of this gripper type were considered. Here are some of these designs:

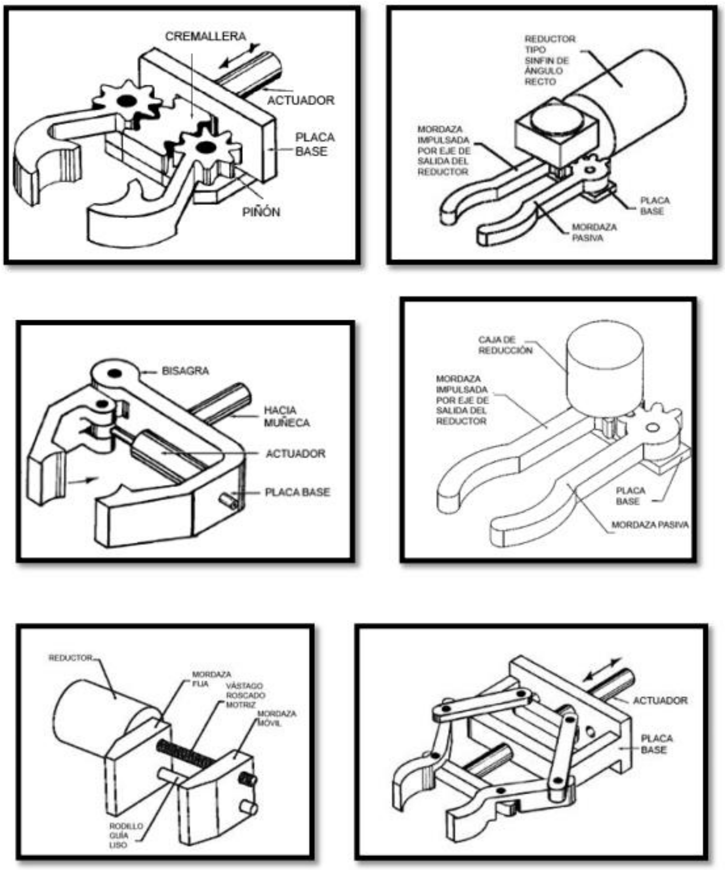

Figure 13: Six different gripper with translation movement

As illustrated in [13], there are numerous types of grippers available. Furthermore, grippers with translational movement are classified into different groups based on the mechanism used to move the gripper:

1. **Linkage Grippers**: Movement occurs solely through attached links without cams, screws, or gears. A well-designed mechanism is crucial to transform the input actuator's motion into gripping action at the output.

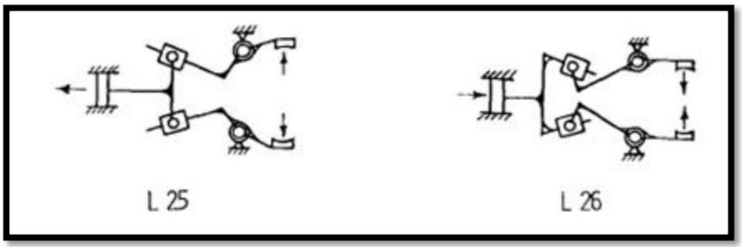

Figure 14: Example of two linkage grippers

2. **Gear and Rack Grippers**: Movement of the input due to gear motion causes connecting links to move, resulting in gripping action at the output link.

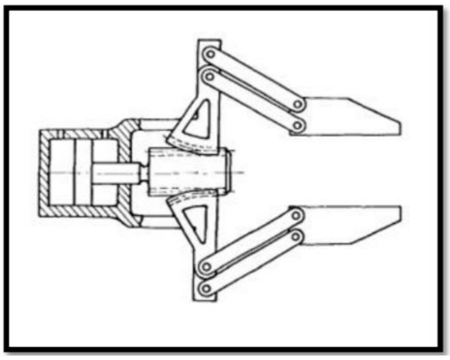

Figure 15; Gear gripper with the motion in the middle

3. **Cam-actuated Grippers**: The reciprocating motion of the cam imparts motion to the follower, causing fingers to produce a grabbing action. Various cam profiles such as constant velocity, circular arcs, and harmonic curves can be employed. This mechanism is like the linkage gripper, but cams are involved.

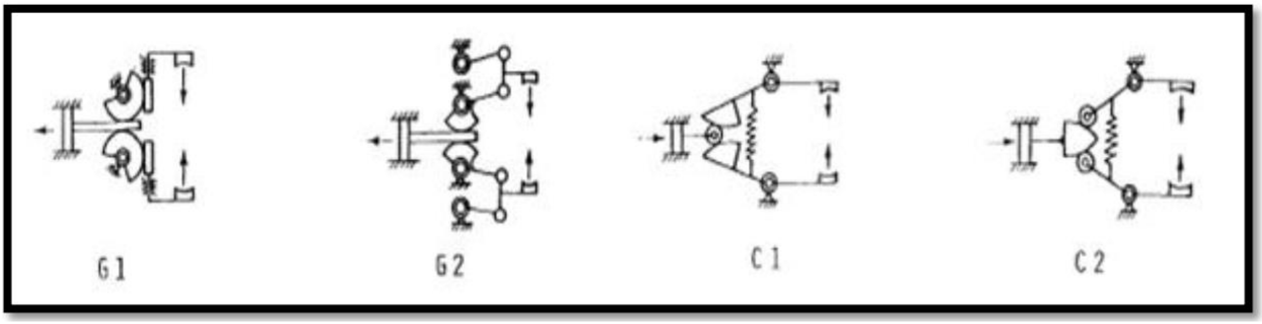

Figure 16: Four different examples of cam-actuated grippers

4. **Screw-driven Grippers**: Operated by turning a screw, which in turn moves connecting links and provides gripping motion at the output. Screw motion can be controlled by a motor attached.

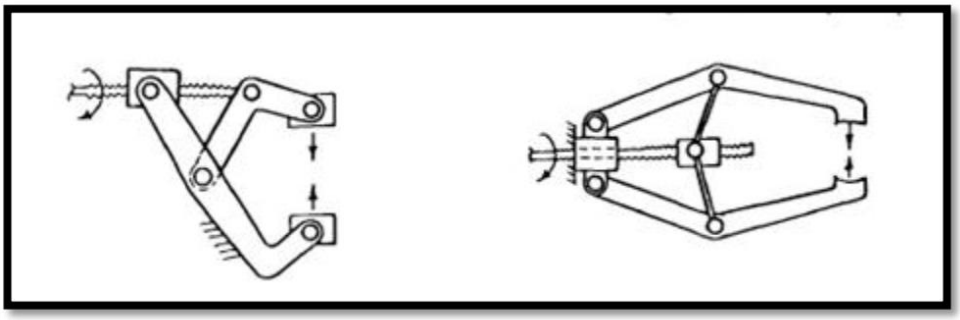

Figure 17: Examples of screw-driven grippers

5. **Rope & Pulley Grippers**: A motor attached to the pulley facilitates the winding and unwinding motion of the rope, thereby initiating gripper action via a connecting link.

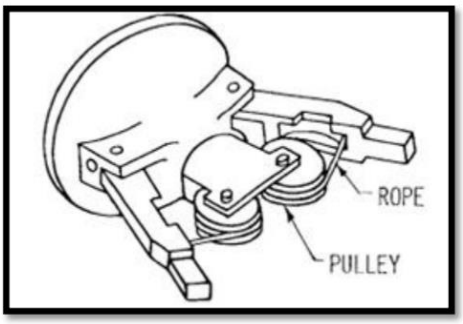

Figure 18: Rope pulley gripper

2. Gripper object of study

The **gear gripper** was chosen because it seemed to be the most cost-effective and practical solution, and it was relatively easy to build. The 2-Finger Gripper has two articulated fingers that each have two joints and three phalanxes per finger:

- Proximal phalanx
- Distal phalanx
- Medial phalanx

as shown in the figure below. The grasp-type gripper has two points of contact with an object. The fingers are under-actuated, meaning they have fewer motors than the total number of joints.

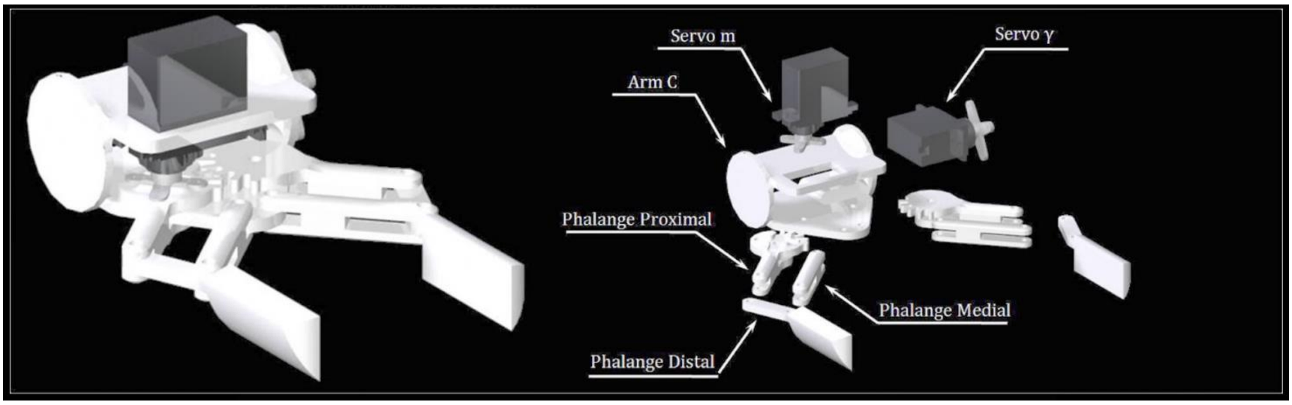

Figure 19: 3D representation of the chosen gripper

A rotary motion of the gears results in a translatory motion of the fingers.

The figure below shows the gripper components that are explained in the next sub-section.

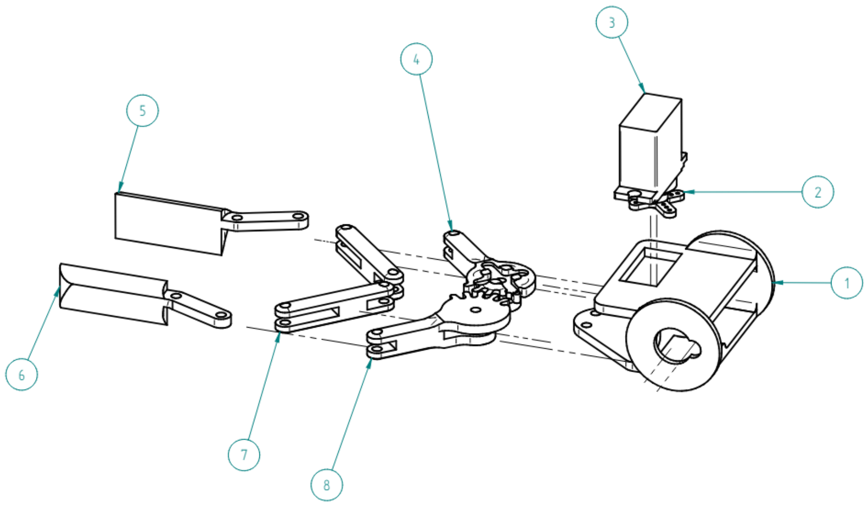

Figure 20: Gripper components

2.1 Analysis of the Gripper

The two fingers of the gripper are symmetrical and have a parallelogram mechanism, two pairs of parallel sides that do not vary in length but do vary in the angle between them.

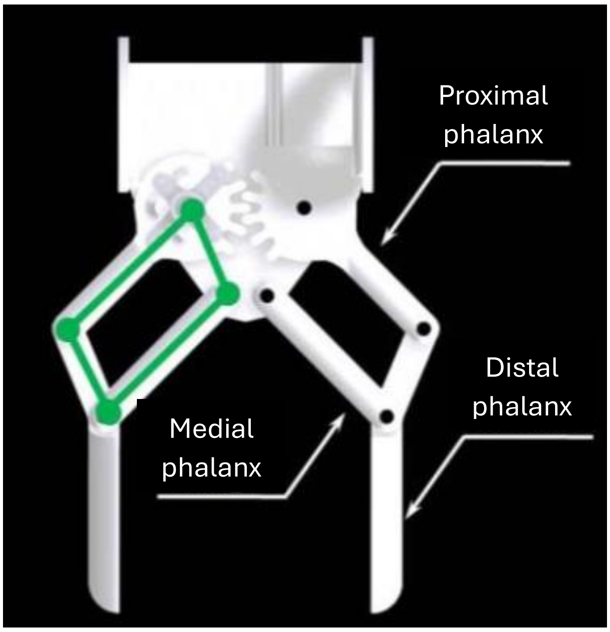

Figure 21: Gripper of study

The gripper consists mainly of two components, namely the **fingers** and the **base**.

Each finger consists of:

- **Proximal phalanx**: is the part that transmits movement and position to the finger. It is attached to the base by an external hinge and, thanks to the gear wheel, transmits the movement to the other phalanx. They are symmetrical, so that both fingers always maintain the same opening angle.

The tooth sizes of the right and left gears must be the same, this is very important for the function of the mechanism.

In a later chapter, the design in SolidWorks of gear wheels will be shown. The ISO formulae defining standardised parameters, dimensions and geometrical characteristics of gear wheels are considered. [6]

- **Medial phalanx**: It has the same length as the proximal phalanx and always moves parallel to it to obtain a parallelogram that varies in its angles but not in its sides; this type of movement allows both fingers to always be parallel.

- **Distal phalanx**: It is the last part of the finger and is used to grasp objects. It is connected to the proximal phalanx and medial phalanx. The two phalanges move so that they are always parallel. They must be carefully designed, the shape and material must be chosen taking into consideration that objects of different shapes and weights will be gripped, a large contact surface allows the gripper to better grasp the object and that there should always be at least two points of contact between the phalanxes and the object to be gripped.

  The distal phalanx was designed to have two main parts: the central part is designed to grasp cylindrical or spherical objects, while the two external parts are intended for objects with 2 or more parallel surfaces. Irregular objects will somehow fit into the center while also having two or more contact points.

- The **base** will serve as the central connection point for all parts of the gripper, except for the two distal phalanges. It's crucial to design the shape of the base so that its upper part is not overly wide, allowing the gripper to close completely.
  This design approach not only prevents contact between the base and the other phalanges but also ensures that the gripper's minimum opening angle is maximized. Conversely, the gripper would only be capable of grasping very large objects.

2.2 Grasping force

During the manufacturing process, it is essential to maintain the stability of the object being handled. It is essential to avoid local or widespread damage to the product at every stage of the production cycle. This requires an adequate grip, calibrated according to the type of object being handled.

Let's call F_G the force necessary to grip an object of mass m, whose general formula, valid for every type of gripper, is:

$$F_g = \frac{m(g + a)}{\mu * n} * S$$

Where:

m: mass of the object to be grasped.

g: gravity acceleration.

a: acceleration in a direction orthogonal to the gripping plane of the gripper's wrist.

μ: coefficient of friction between the "fingertips" of the gripper and the object.

n: number of gripper fingers.

S: *safety factor*.

The choice of safety margins depends on the type of movement performed [4]:

- Safety factor equal to 2 for normal applications.
- Safety factor equal to 3 for movement on multiple axes with low acceleration and braking.
- Safety factor equal to 4 for strong accelerations and sudden impacts.

For our case study we chose a value of S equal to 2.

The forces that the cylindrical or parallel-faced object exchanges with the gripper's fingers are shown below:

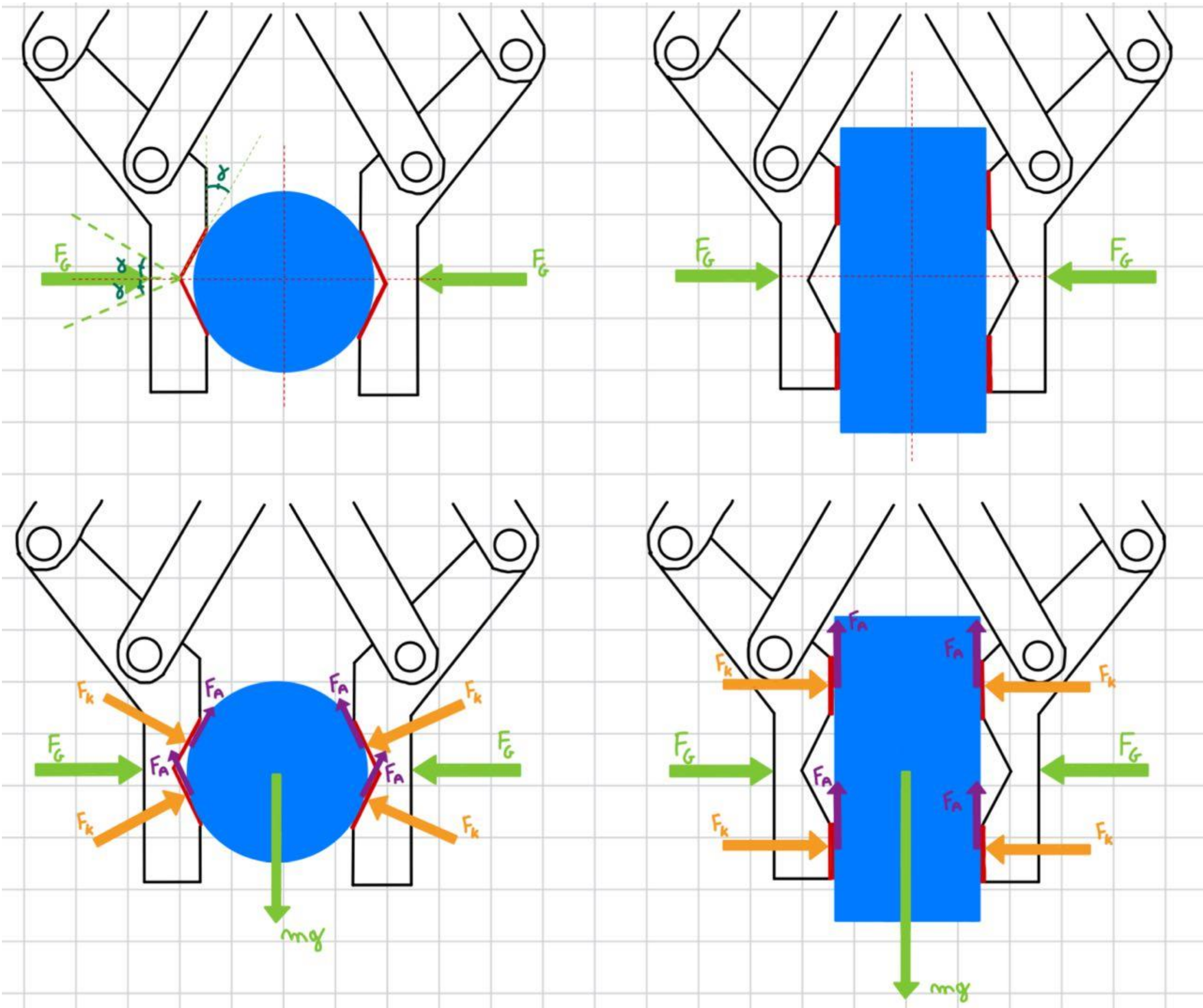

Figure 22: Representations of grasping forces

3. Kinematic analysis

It is possible to schematise and represent the gripper mechanism in the following way:

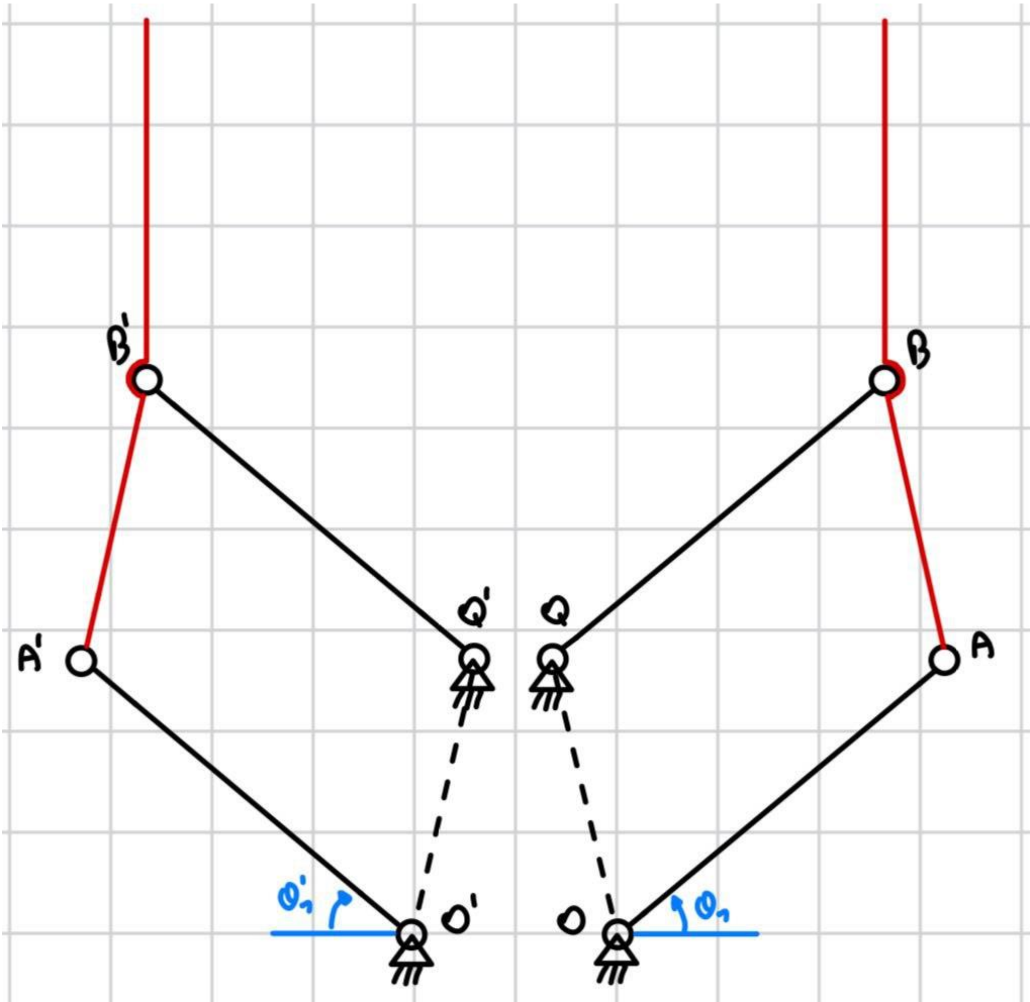

Figure 23: Representation of the gripper mechanism

The *geometric study* is as follows:

- 6 rigid => 18 degrees of freedom
- 4 external hinges => -8 degrees of freedom
- 4 rotoidal pairs => -8 degrees of freedom

So, we have 2 residual degrees of freedom, 1 Lagrangian parameter for each finger (ϑ_1 e ϑ_1').

We can easily see the symmetry between the left and right sides; therefore, the relationship between the two Lagrangian parameters is obvious: $\vartheta_1' = -\vartheta_1$.

Due to the symmetry of the mechanism, it is possible to assess the kinematics of the mechanism by considering only the right-hand side of the gripper. Given the following figure:

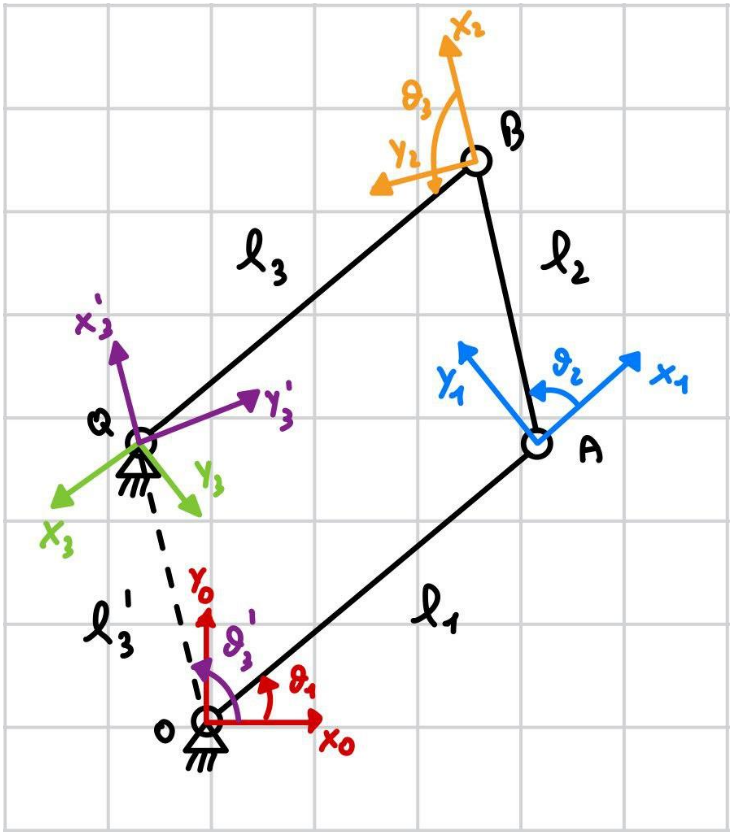

Figure 24: Right-hand side of the gripper

A kinematic model of a mechanism can be evaluated using the method of homogeneous transformation matrices, which uses the Denavit-Hartenberg (DH) convention. Robotics is one of the fields in which this method is widely used, but it can be applied to all types of mechanical mechanisms and systems.

It should be specified that the mechanism under study can be traced back to a ***parallelogram mechanism***, where there is a closed chain. Joint number 4 was chosen as the shear joint and the triads integral to the arms were determined accordingly.

In the search for DH parameters, the presence of a fourth arm was considered. The latter is not actually present, as it imaginarily connects the two outer hinges.

The DH parameters are specified in the following tables:

Link	a_i	α_i	d_i	ϑ_i
1	l_1	0	0	ϑ_1
2	l_2	0	0	ϑ_2
3	l_3	0	0	ϑ_3

Link	a_i	α_i	d_i	ϑ_i
3'	l_3'	0	0	ϑ_3'

Where the first table refers to the open chain formed by links 1, 2 and 3. While the second refers to the chain formed by the imaginary link 3' alone, which forms the second open chain.

To find the kinematic function, remember that the general form of the homogeneous transformation matrix is:

$$T_i^{i-1}(q_i) = \begin{bmatrix} c\vartheta_i & -s\vartheta_i * c\alpha_i & s\vartheta_i * s\alpha_i & a_i * c\alpha_i \\ s\vartheta_i & c\vartheta_i * c\alpha_i & -c\vartheta_i * s\alpha_i & a_i * s\alpha_i \\ 0 & s\alpha_i & c\alpha_i & d_i \\ 0 & 0 & 0 & 1 \end{bmatrix}$$

Thus, for the first open chain, the homogeneous transformation matrix is obtained by post-multiplying the individual transformation matrices, as shown below:

$$T_3^0(q) = T_1^0(q_1) * T_2^1(q_2) * T_3^2(q_3)$$

Thus:

$$T_3^0(q) = \begin{bmatrix} c_1 & -s_1 & 0 & l_1c_1 \\ s_1 & c_1 & 0 & l_1s_1 \\ 0 & 0 & 1 & 0 \\ 0 & 0 & 0 & 1 \end{bmatrix} \begin{bmatrix} c_2 & -s_2 & 0 & l_2c_2 \\ s_2 & c_2 & 0 & l_2s_2 \\ 0 & 0 & 1 & 0 \\ 0 & 0 & 0 & 1 \end{bmatrix} \begin{bmatrix} c_3 & -s_3 & 0 & l_3c_3 \\ s_3 & c_3 & 0 & l_3s_3 \\ 0 & 0 & 1 & 0 \\ 0 & 0 & 0 & 1 \end{bmatrix} =$$

$$= \begin{bmatrix} c_{123} & -s_{123} & 0 & l_1c_1 + l_2c_{12} + l_3c_{123} \\ s_{123} & c_{123} & 0 & l_1s_1 + l_2s_{12} + l_3s_{123} \\ 0 & 0 & 1 & 0 \\ 0 & 0 & 0 & 1 \end{bmatrix}$$

Where $q = \begin{bmatrix} \vartheta_1 \\ \vartheta_2 \\ \vartheta_3 \end{bmatrix}$.

In contrast, for the second open chain, the homogeneous transformation matrix is as follows:

$$T_{3'}^{0}(q') = \begin{bmatrix} c_{3'} & -s_{3'} & 0 & l_{3'}c_{3'} \\ s_{3'} & c_{3'} & 0 & l_{3'}s_{3'} \\ 0 & 0 & 1 & 0 \\ 0 & 0 & 0 & 1 \end{bmatrix}$$

Where $q' = \vartheta_3'$.

Finally, position and orientation constraints must be imposed to satisfy the closure equation.

Orientation constraints are met regardless of q and q'. On the other hand, position constraints must be imposed:

$$\vec{O_3^0}(q) = \vec{O_{3'}^0}(q')$$

$$\begin{bmatrix} l_1c_1 + l_2c_{12} + lc_{123} \\ l_1s_1 + l_2s_{12} + l_3s_{123} \\ 0 \end{bmatrix} = \begin{bmatrix} l_{3'}c_{3'} \\ l_{3'}s_{3'} \\ 0 \end{bmatrix}$$

Where the vectors $\vec{O_3^0}(q)$ e $\vec{O_{3'}^0}(q')$ represent respectively the position of the origin of the reference system $O_3X_3Y_3Z_3$ and $O_{3'}X_{3'}Y_{3'}Z_{3'}$ with respect to $O_0X_0Y_0Z_0$.

Imposing the physical constraints of the mechanism:

$$\begin{cases} l_1 = l_3 \\ l_2 = l_{3'} \\ \vartheta_{3'} = \vartheta_1 + \vartheta_2 \end{cases}$$

The following non-linear system is obtained to be solved:

$$\begin{cases} \cos(\vartheta_1) + \cos(\vartheta_1 + \vartheta_2 + \vartheta_3) = 0 \\ \sin(\vartheta_1) + \sin(\vartheta_1 + \vartheta_2 + \vartheta_3) = 0 \end{cases}$$

For the resolution of the system, we can consider varying the angle ϑ_1 in the range of maximum variation, which was determined through the data in the studies [5] and [7]. Solving this non-linear system yields the angle variations ϑ_2 and ϑ_3 as a function of ϑ_1.

Using MATLAB's `fsolve` function, the following results were obtained:

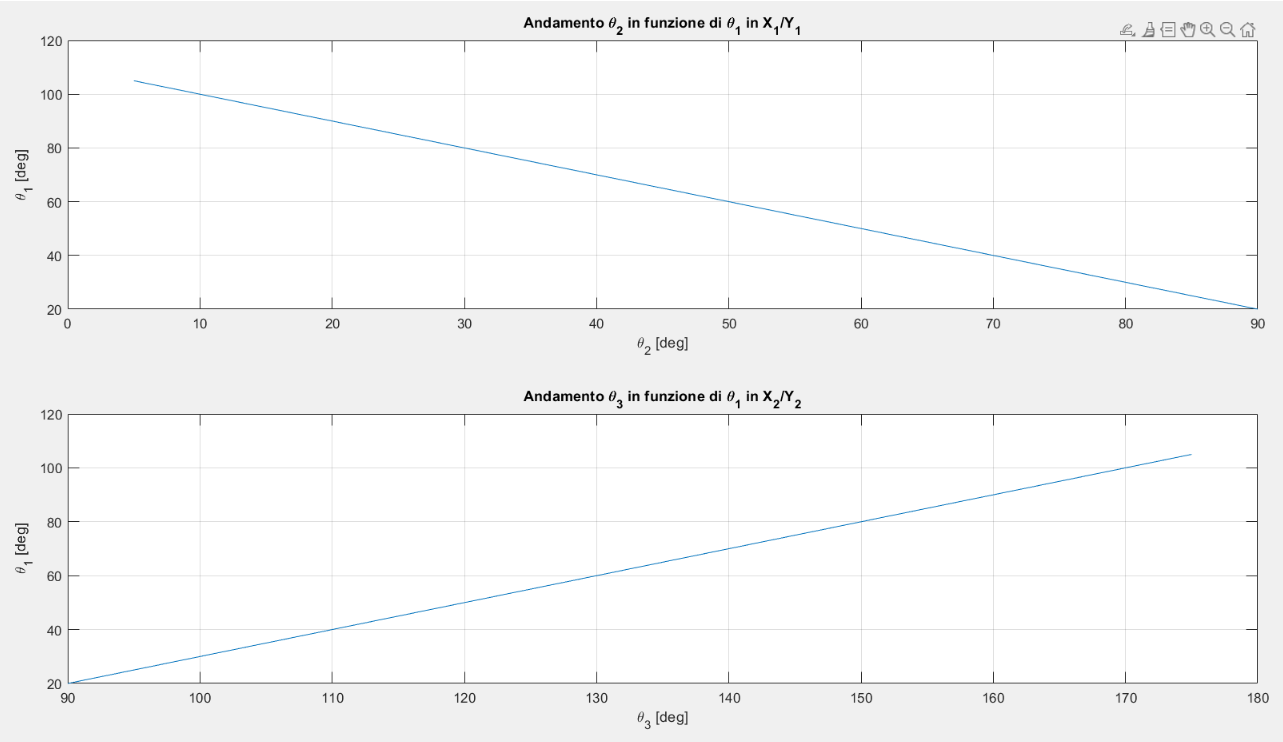

Figure 25: Angle trend in MATLAB

The first subplot shows the variation of angle ϑ_2 as a function of ϑ_1 in the reference system of the second joint X_1Y_1.

The second subplot shows the variation of angle ϑ_3 as a function of ϑ_1 in the reference system of the third joint X_2Y_2.

The variation is linear for both angles, in fact, for a decrease of the angle ϑ_1, which corresponds to the opening of the gripper, the angle ϑ_2 increase.

Instead, as the angle ϑ_1 increase, which corresponds to the gripper closure, angle ϑ_3 increase.

In general, the angle ϑ_1 is inversely proportional to ϑ_2 and directly proportional to ϑ_3.

3.1 Trajectory

Since it is a parallelogram configuration, each point on the l_2 link has the same velocity and acceleration. Furthermore, the angular velocity is zero. Therefore, it can be stated that the l_2 link is characterised by a translatory motion with a curvilinear trajectory.

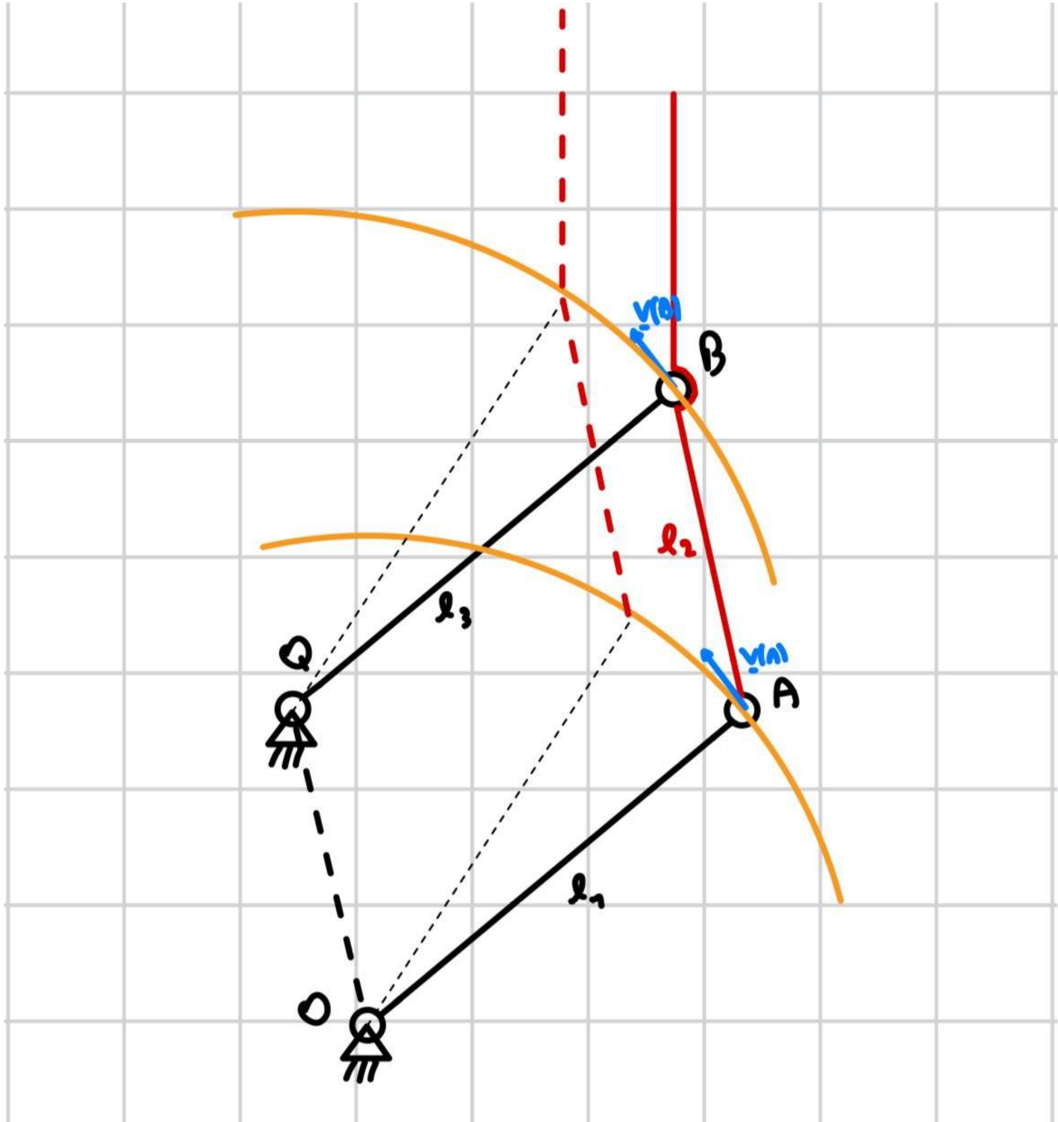

Figure 26: Trajectory of the parallelogram mechanism

The yellow curves show the trajectories of point A and B.

In the following paragraphs, the trajectory is analysed in SolidWorks with the maximum and minimum angles that the parallelogram mechanism can reach. From here, the value of the maximum distance between the gripper phalanxes was also evaluated. Designing the Robotic Gripper Model in SolidWorks

4. Designing the Robotic Gripper Model in SolidWorks

In this chapter, we will delve into the process of developing a SolidWorks model for the analysed robotic gripper, providing a detailed breakdown of the modelling process. We will start by explaining the reasons for choosing to use SolidWorks. Then, we will present each component of the gripper, describing its design and function. Finally, we will demonstrate how these parts were assembled to create the complete mechanism.

SolidWorks is an advanced 3D computer-aided design (CAD) software widely used for precise modelling, simulation, and analysis of mechanical systems, chosen for this project for its widespread adoption and powerful functionalities in professional engineering. This software has allowed us to visualize the design in a three-dimensional space, make iterative improvements efficiently, and perform motion and force analysis. Thanks to SolidWorks, we were able to precisely model the individual components of the robotic gripper, simulate their interactions, and ensure that all parts functioned together as intended.

It is important to emphasise that the unit system set is MMGS (millimetre, gram, second).

For the design of the gripper, we started by creating a sketch of only the right side of the mechanism [see Figure 27], considering that its symmetry makes it unnecessary to include the left side.

The dimensions of the sketch were determined based on the technical document [5]. The sides of the parallelogram, namely the proximal phalanx and the medial phalanx, measure 20mm and 35mm respectively, the gripping finger, or distal phalanx, measures 40mm, and the fixed angle was chosen to be 70°.

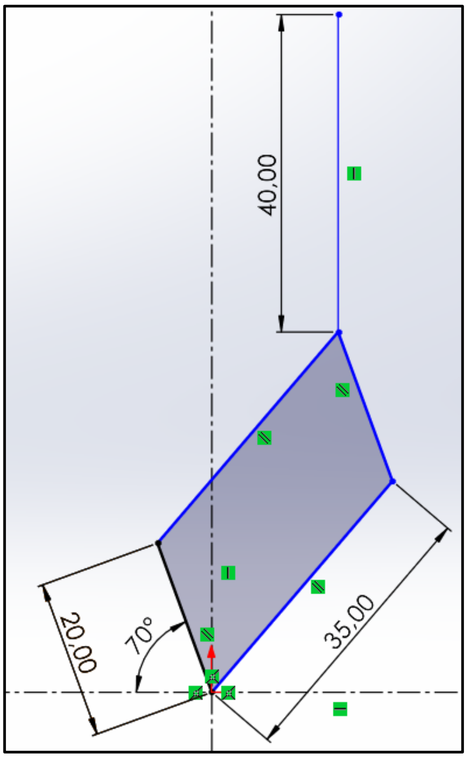

Figure 27: Sketch of the right side of the mechanism

After defining the sketch, we evaluated the movement of the mechanism to ensure it behaved as expected. Once we confirmed that the movement met our expectations, we proceeded to develop the individual parts of the mechanism.

4.1 Base

To model the base, we started by drawing a sketch and then performed an extrusion to obtain the part in 3D.

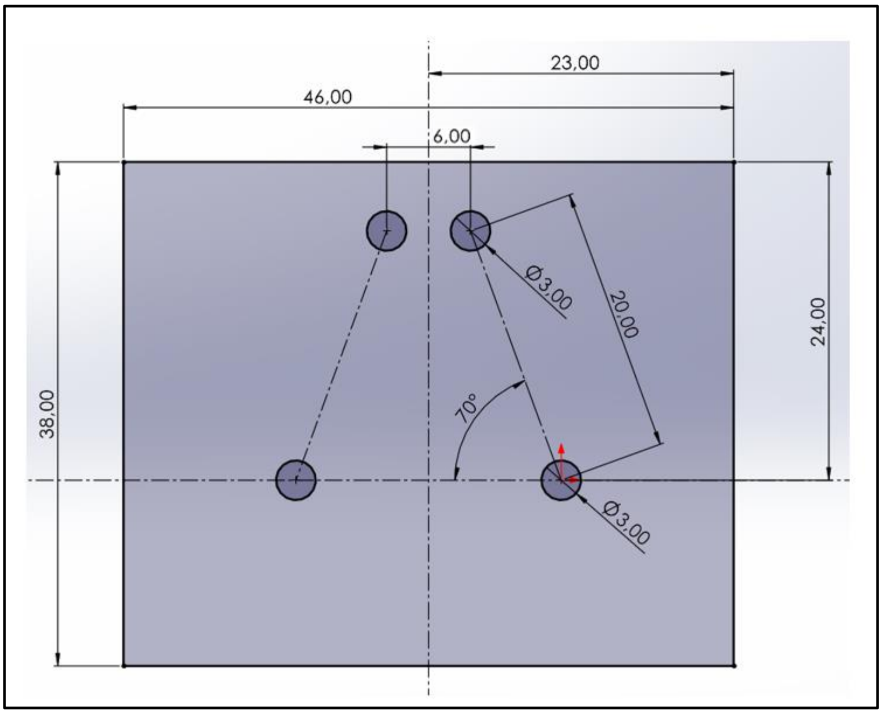

Figure 28: Base sketch

Next, we created a sketch for cutting to remove excess material and prevent the base from unwanted contact with other mechanism components.

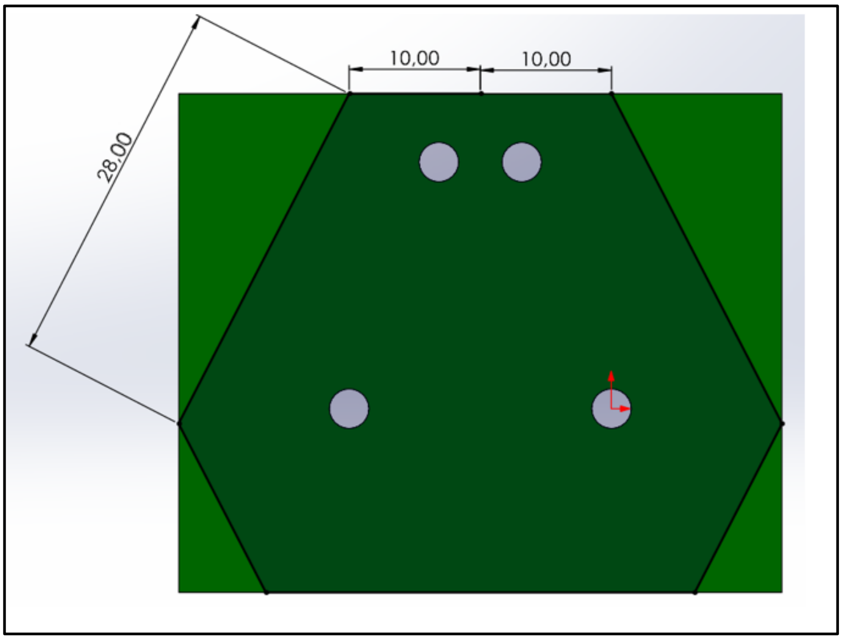

Figure 29: Base sketch before extrusion

Finally, we applied fillets to round off the edges, reduce bulk and save material. This component is shown in the figure below:

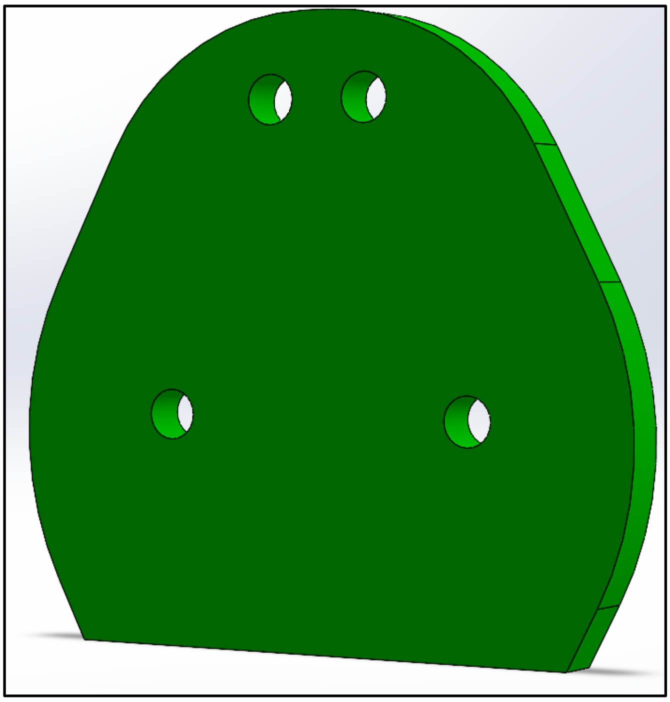

Figure 30: Extruded Base

4.2 Link 1

We initiated by sketching the gear wheel and straight slot.

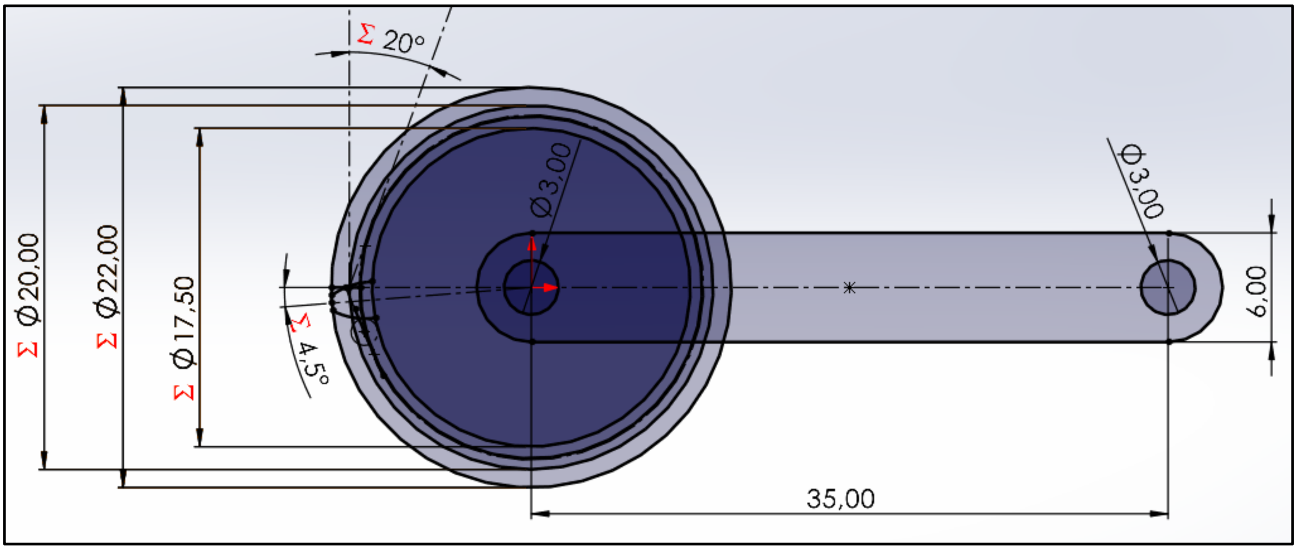

Figure 31: Link 1 sketch

The gear wheel was designed with a module of 1 and 20 teeth, resulting in a primitive circumference diameter of 20 mm. This is crucial as it ensures that, upon assembling link 1 and its symmetric counterpart at the base, the two gear wheels are correctly engaged. Specifically, in the following figure, all parameters defined for designing the gear wheel are depicted:

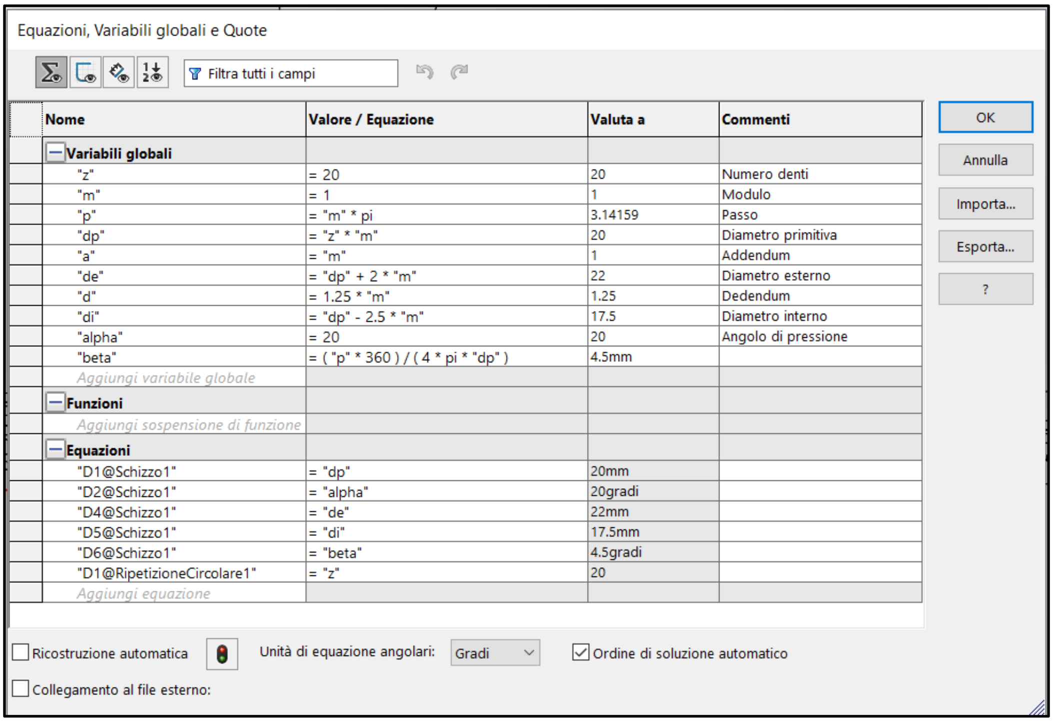

Equazioni, Variabili globali e Quote

Nome	Valore / Equazione	Valuta a	Commenti
Variabili globali			
"z"	= 20	20	Numero denti
"m"	= 1	1	Modulo
"p"	= "m" * pi	3.14159	Passo
"dp"	= "z" * "m"	20	Diametro primitiva
"a"	= "m"	1	Addendum
"de"	= "dp" + 2 * "m"	22	Diametro esterno
"d"	= 1.25 * "m"	1.25	Dedendum
"di"	= "dp" - 2.5 * "m"	17.5	Diametro interno
"alpha"	= 20	20	Angolo di pressione
"beta"	= ("p" * 360) / (4 * pi * "dp")	4.5mm	
Aggiungi variabile globale			
Funzioni			
Aggiungi sospensione di funzione			
Equazioni			
"D1@Schizzo1"	= "dp"	20mm	
"D2@Schizzo1"	= "alpha"	20gradi	
"D4@Schizzo1"	= "de"	22mm	
"D5@Schizzo1"	= "di"	17.5mm	
"D6@Schizzo1"	= "beta"	4.5gradi	
"D1@RipetizioneCircolare1"	= "z"	20	
Aggiungi equazione			

Figure 32: Gear parameters

Subsequently, we performed extrusion and made several cuts: a lateral cut to prevent link 1 from unwanted contact with the base and link 2; a cut at the rear part of the gear wheel to remove excess material; a cut to eliminate excess teeth from the gear wheel.

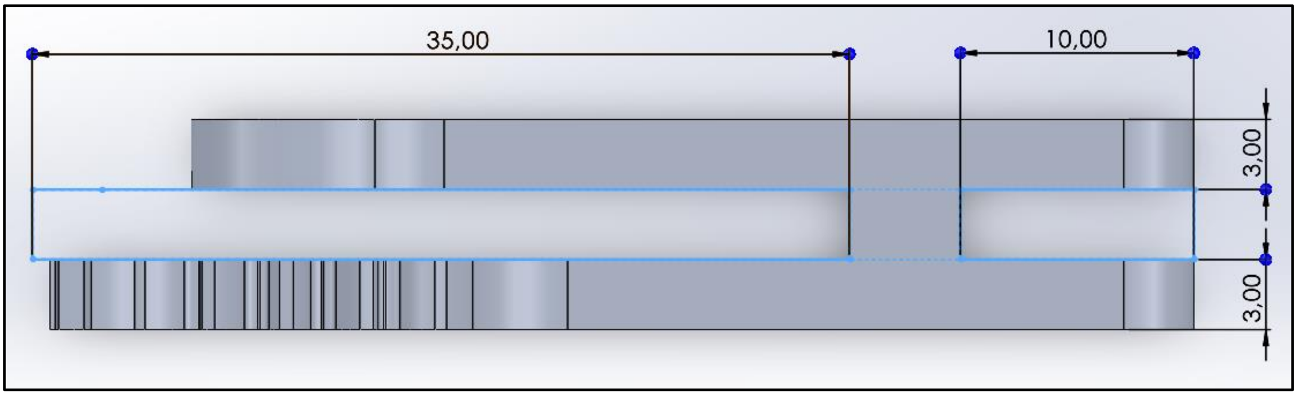

Figure 33: Link 1 - Lateral view

Finally, we applied fillets to enhance aesthetics and reduce stress concentrations. This component is shown in the following figure:

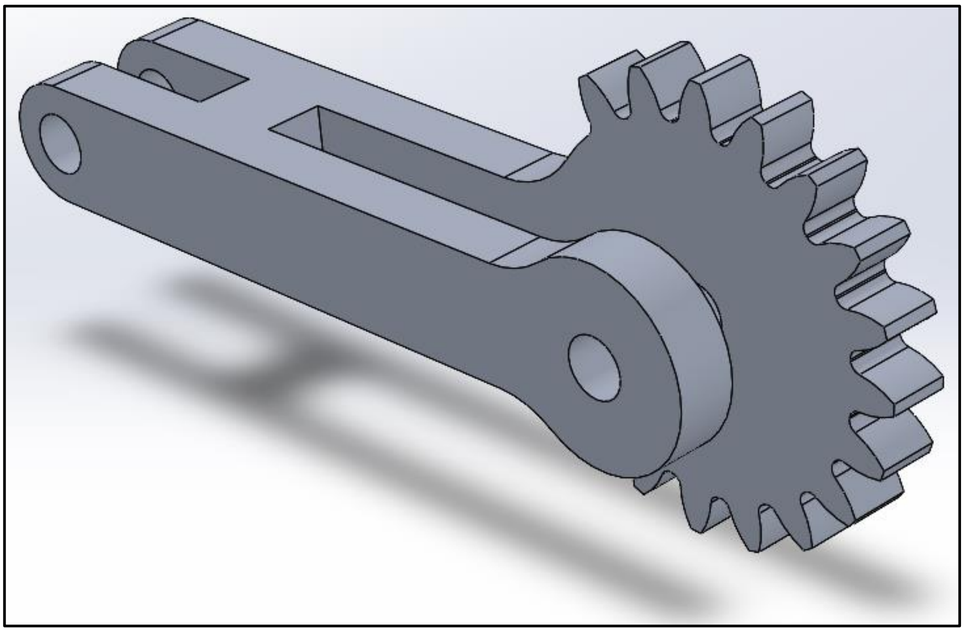

Figure 34: Link 1 - Back view

4.3 Link 2

The modelling of link 2 is characterized by the stages of sketching, extrusion, and filleting.

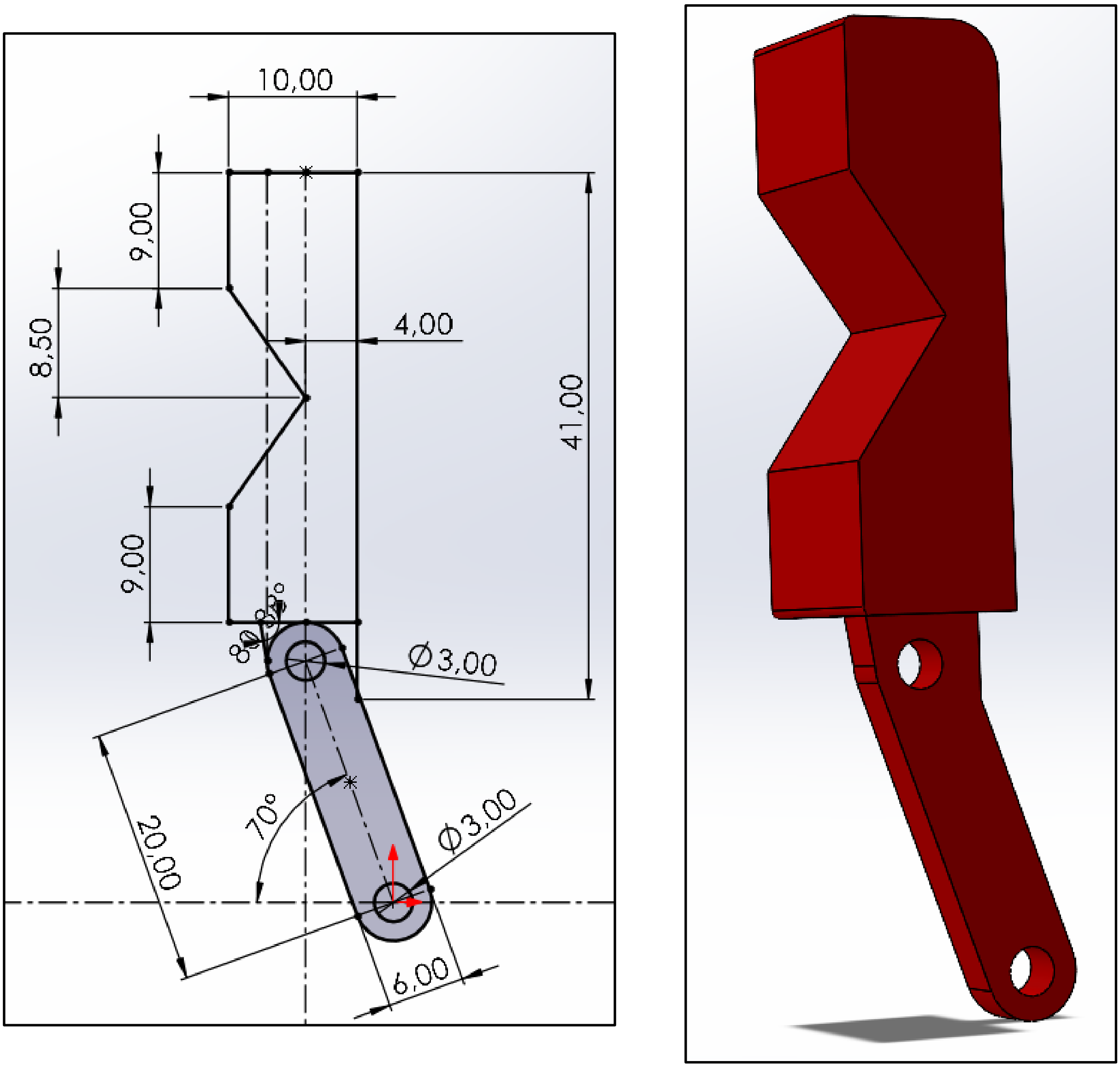

Figure 35: Link 2 - Sketch and extrusion

The shape imposed on the component is designed to better accommodate objects of different shapes and sizes, providing multiple gripping points. The 70-degree angle shown on the sketch is critical to the functionality of the gripper, allowing effective gripping under different orientations and minimising the possibility of slipping. In addition, the thickness and length of the component allows it to withstand specific forces without deforming. This design allows the gripper to grip the object firmly without slipping.

4.4 Link 3

For this component, we simply sketched a Straight Slot, extruded it and cut the side to prevent link 3 from undesired contact with other components.

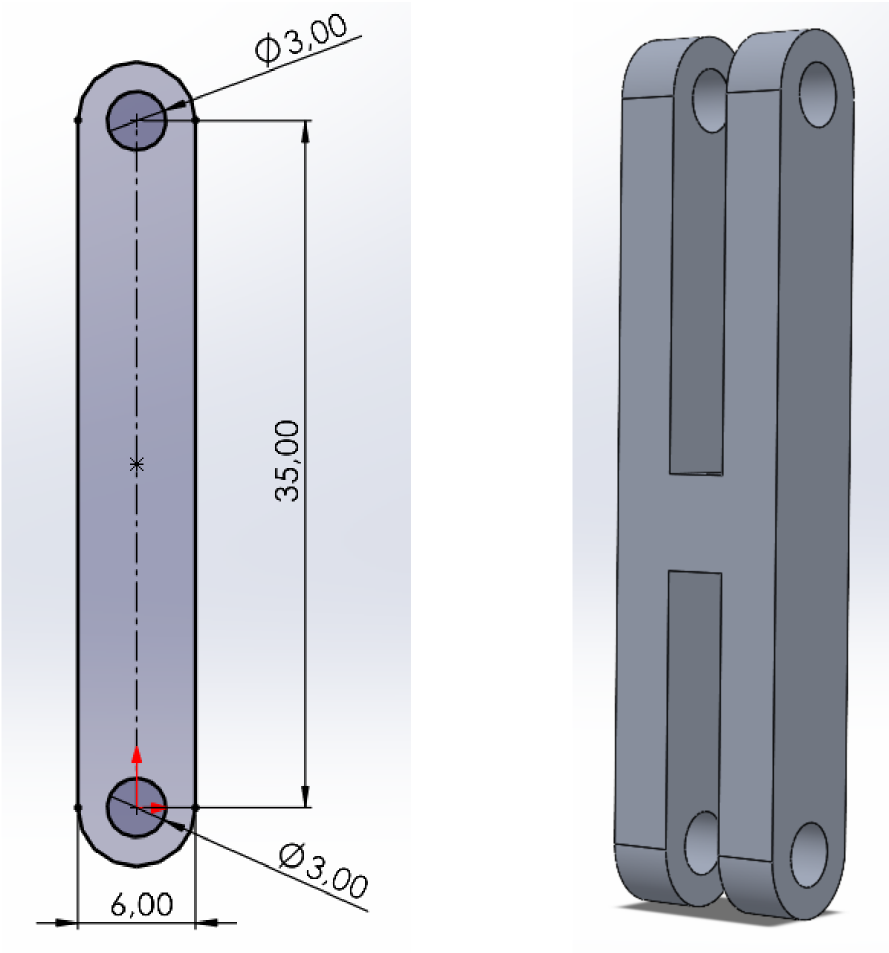

Figure 36: Link 3 - Sketch and extrusion

4.5 Assembly

After completing the design of the gripper components. We moved on to the assembly of the gripper. The following couplings were defined:

- Coincident Mate Link 1 (L) and Base;
- Coincident Mate Link 2 (L) and Link 2 (L);
- Coincident Mate Base and Link 3 (L);
- Coincident Mate Link 2 (L) and Link 3 (L);
- Coincident Mate Link 1 (R) and Base;
- Coincident Mate Link 1 (R) and Link 2 (R);
- Coincident Mate Base and Link 3 (R);
- Coincident Mate Link 2 (R) and Link 3 (R);
- Gear Mate Link 1 (R) and Link 1 (S);

In SolidWorks it results:

Figure 37: Mates

An attempt was made to minimise the presence of redundancies by using as few couplings as possible without compromising the functioning of the mechanism.

The complete gripper is shown in the following figures:

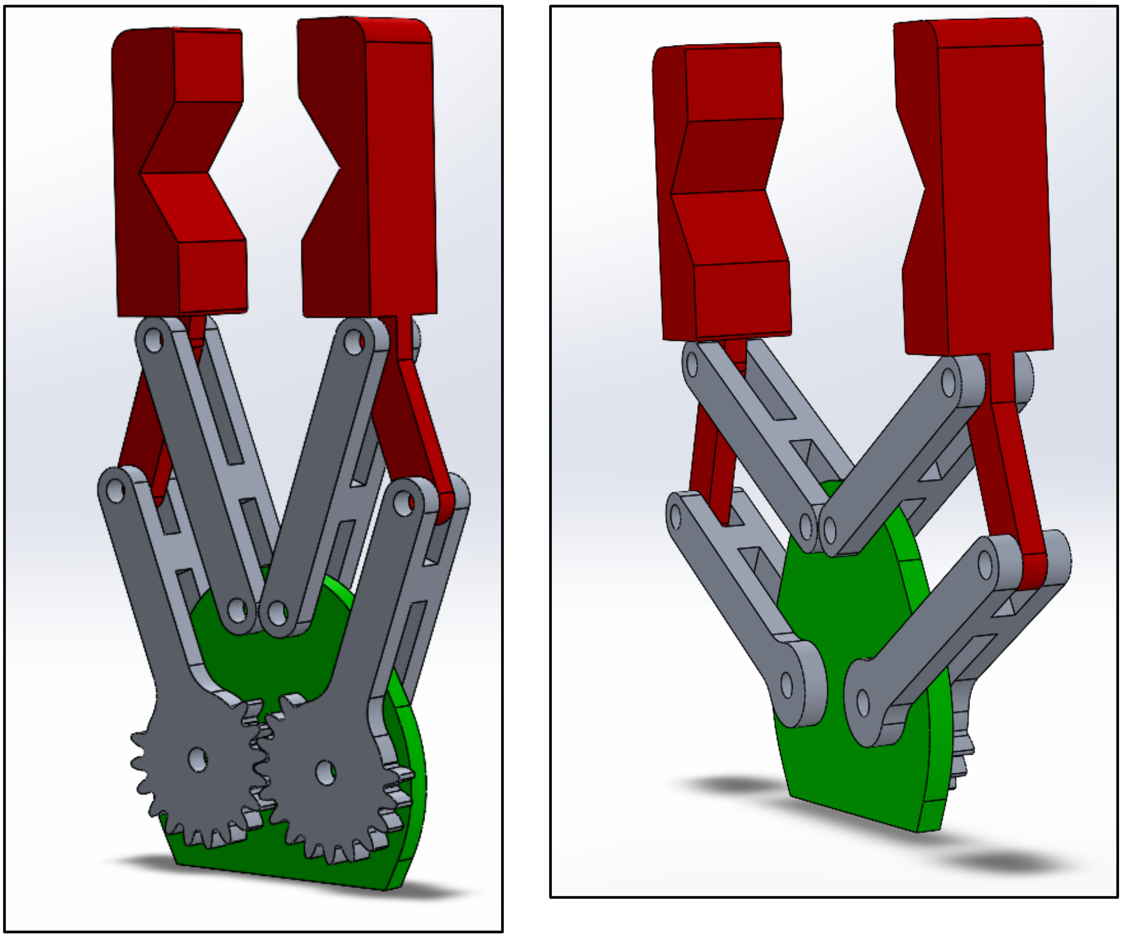

Figure 38: Assembled gripper – Front and Back view

5. Kinematic Analysis in SolidWorks

A motion analysis was carried out in SolidWorks to verify consistency with the kinematic study carried out previously, during which the trends of ϑ_2 and ϑ_3 were evaluated as the angle ϑ_1 varied.

The angles in question are shown in the figure below:

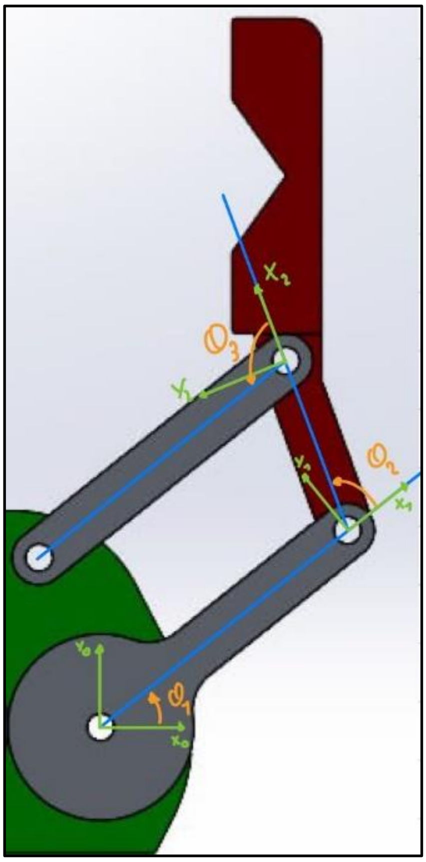

Figure 39: Angles in SolidWorks

The first step in motion analysis in SolidWorks was to set a rotary motor at a speed of $12\ rpm$ on Link 1 (R).

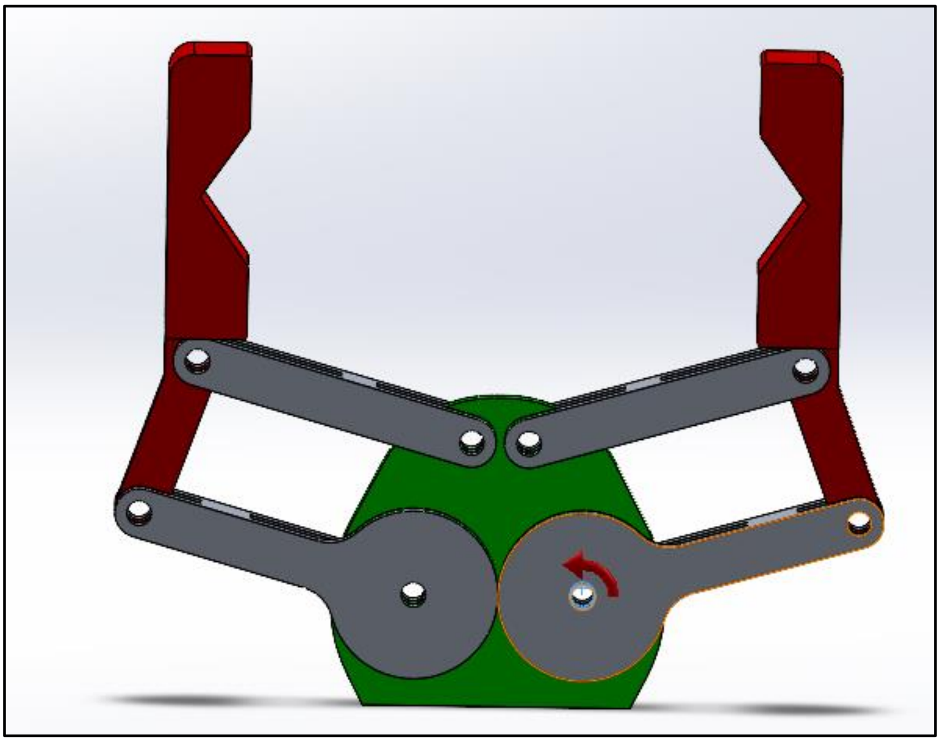

Figure 40: Motor in motion analysis

Subsequently, the variation of angles ϑ_1, $\pi - \vartheta_2$ e $\pi - \vartheta_3$ were evaluated using the SolidWorks tool 'Results and Graphs'. The data from the graphs were exported directly from SolidWorks into three Excel files, respectively.

To consolidate all information in one document [8], a new Excel file was generated containing all data extracted from SolidWorks. In this, the data of how ϑ_2 and ϑ_3 vary over time was obtained. Subsequently, the variation of ϑ_2 and ϑ_3 as ϑ_1 varies was evaluated.

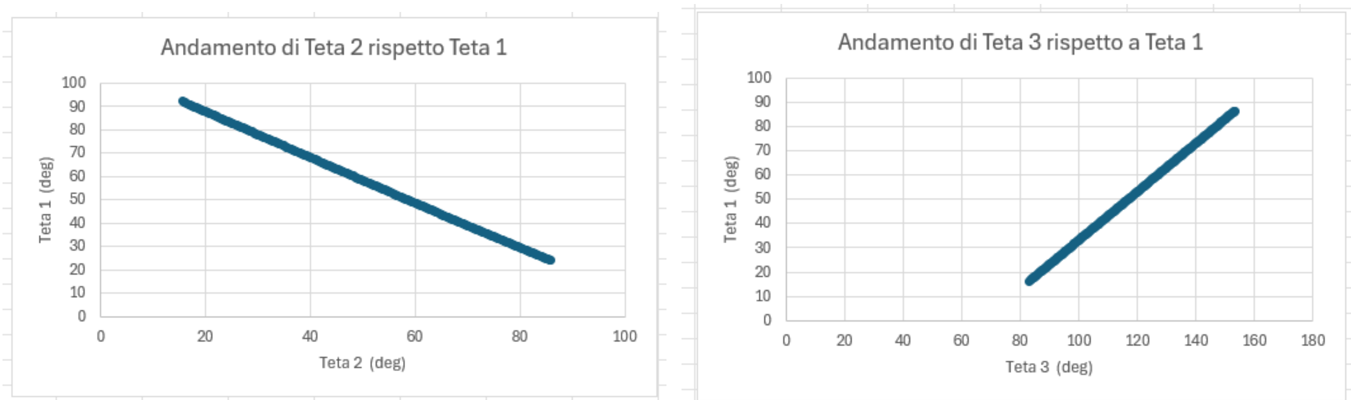

Figure 41: Trend of angles ϑ_1 and ϑ_2

Comparing these graphs with those obtained from the kinematic study done earlier, it can be said that the results coincide.

5.1 Trajectory in SolidWorks

The following figure shows the trajectory of the gripping joints and its minimum opening due to the contact of the two Links 3:

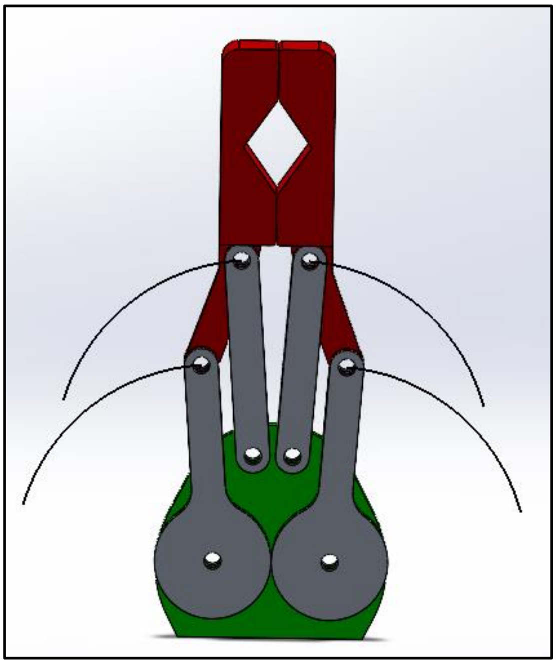

Figure 42: Trajectory in SolidWorks

The maximum opening of the gripper is due to the contact between Link 2 and Link 3, Link 2 being parallel to the gripper bearing surface:

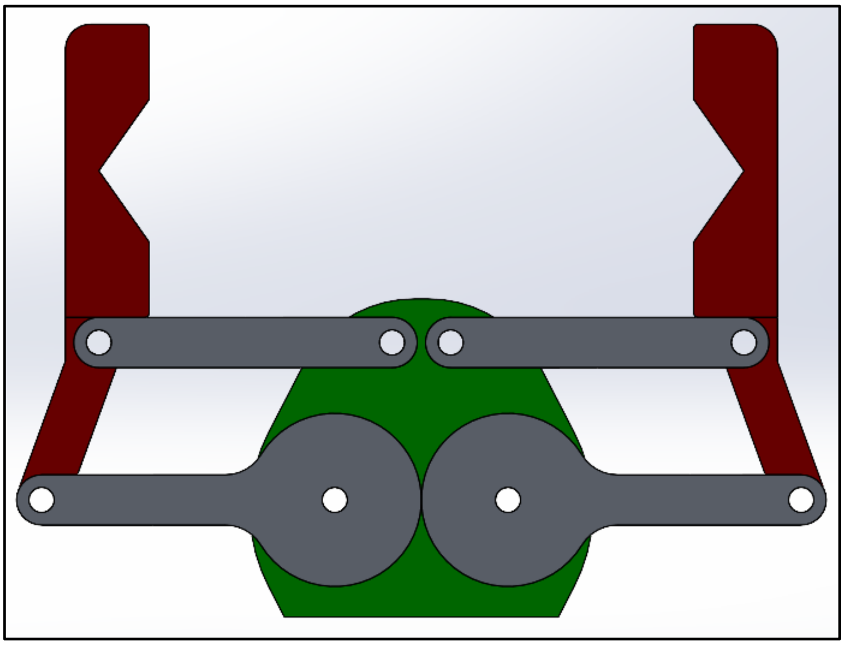

Figure 43: Maximum opening

From the motion analysis done in SolidWorks, the minimum and maximum values of the ϑ_1, ϑ_2 e ϑ_3 angles can be assessed:

$Angles$	$Minimum$	$Maximum$
ϑ_1	$0°$	$86°$
ϑ_2	$24°$	$110°$
ϑ_3	$70°$	$156°$

$Min\ phalanx\ distance$	$0\ mm$
$Max\ phalanx\ distance$	$64\ mm$

6. Force analysis in SolidWorks

After carrying out the kinematic analysis in SolidWorks, we wanted to analyse the trend of the torque T at the variation of the force value F_G, while keeping the angle value ϑ_1 constant.

To assess this characteristic, the force F_G was applied only when the last gripper phalanges are in contact, thus simulating the gripping of an object in the middle.

A rotary motor was then applied to the right wheel with the movement type set to 'Distance'. The gripper will move until it closes.

Once this configuration is achieved, two F_G forces are applied, one for each finger of the gripper.

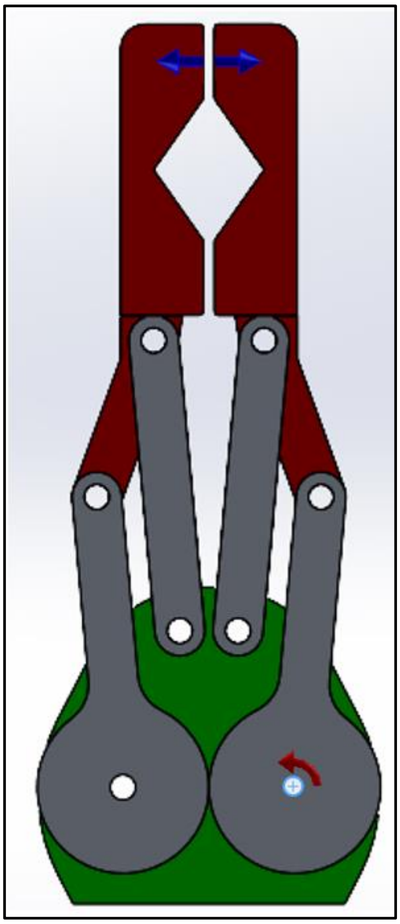

Figure 44: Force analysis configuration

By varying the F_G force, we then evaluated the torque the motor delivered to maintain the position, and thus the grip. Recalling the force equation:

$$F_G = \frac{m(g + a)}{\mu * n} * S$$

the following values were used:

- m: mass of the object ranging from $10gr$ to $100gr$ in steps of $10gr$;
- $g = 9{,}81\ m/s^2$;
- $a = 0\ m/s^2$: it is assumed that there is no movement of the gripper in the orthogonal direction;
- $\mu = 0{,}25$: metal-to-metal contact;
- $n = 2$;
- $S = 2$.

The torque values obtained in SolidWorks were then imported into MATLAB where, in addition to the plot relating the force F_G to the torque T required to hold the object, the relationship between the force F_G and the mass m of the object is also plotted.

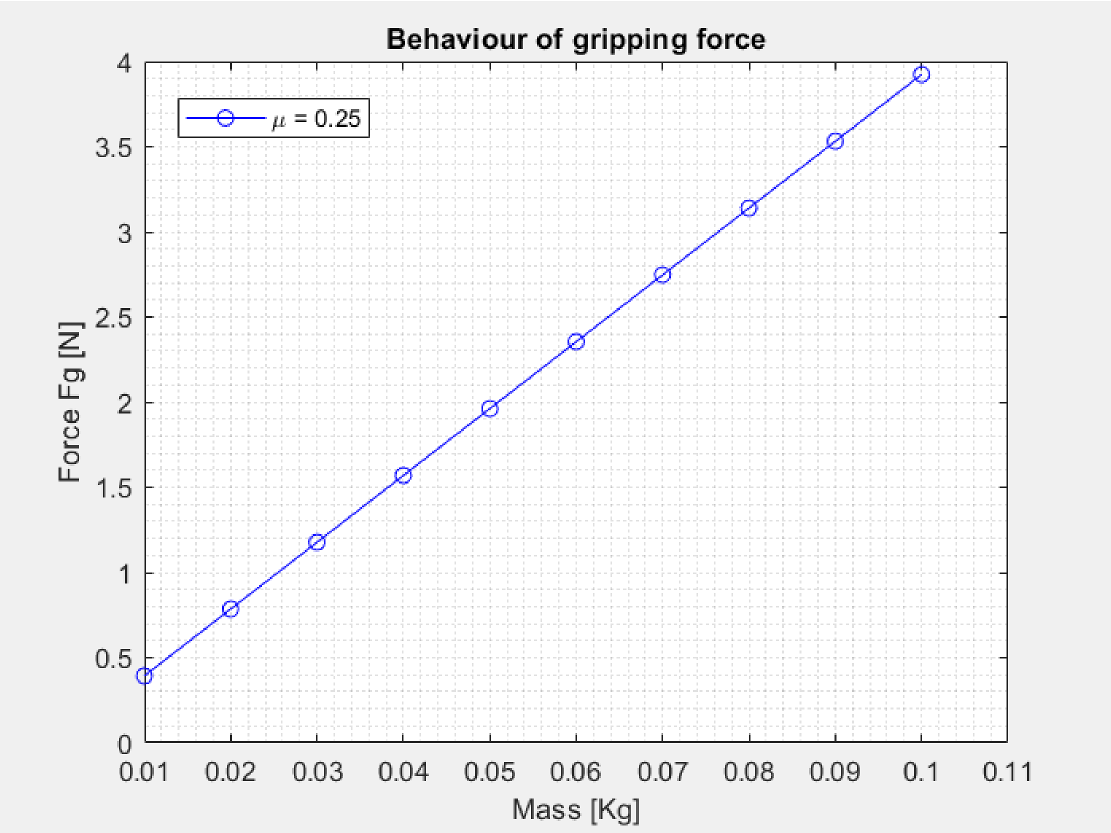

Figure 45: Behaviour of gripping force wrt mass

As can be seen from figure [45], the value of the forceF_G increases as the mass increases, as expected since the force is directly proportional to the mass of the object.

However, it should be remembered that the object varies only in its mass and not in its size. In fact, a different size corresponds to a different configuration of the parallelogram mechanism, and as we have seen from the theoretical study, a different configuration, hence a different ϑ_1 angle, corresponds to a different torque value.

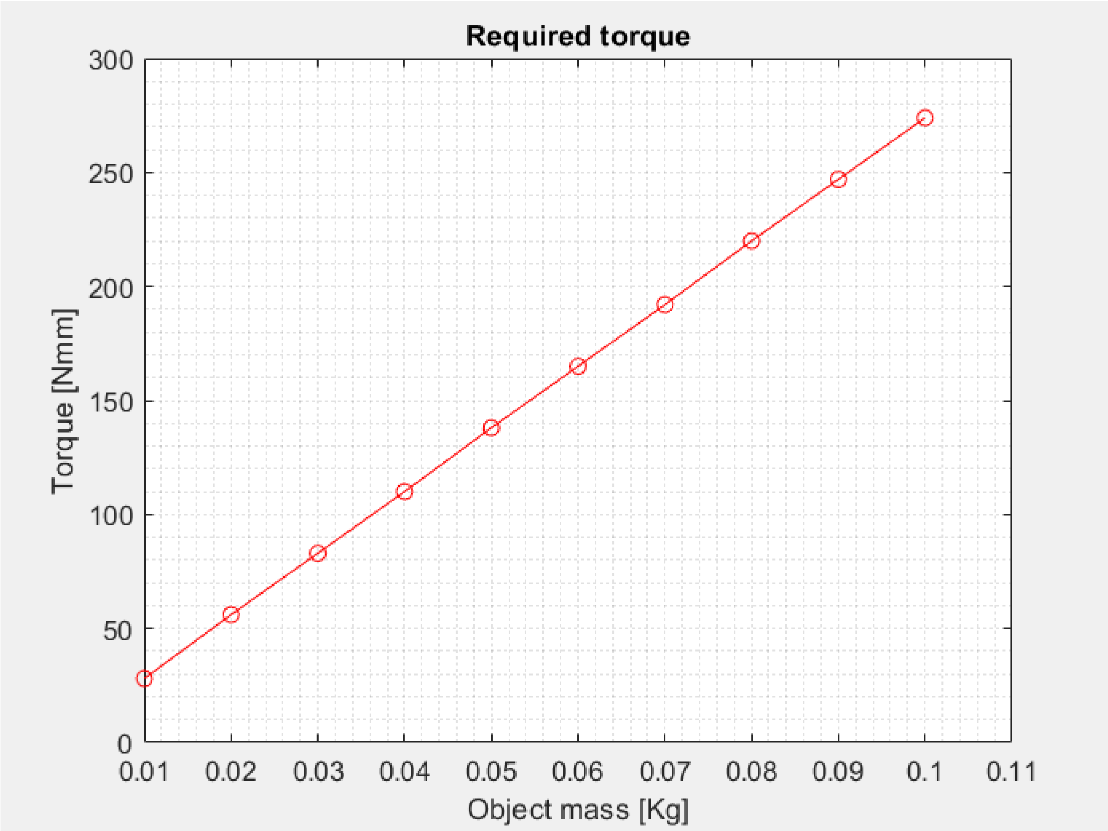

Figure 46: Required torque

Again, the relationship is directly proportional; an object with a greater mass requires a higher torque to maintain equilibrium.

7. Simulations

This section describes the different simulations carried out to assess the quality of the designed gripper. Different configurations of the mechanism with objects of different shapes and sizes were considered.

A constant torque of $150\ N \cdot mm$ was set for each simulation in order to assess how the contact force between object and gripper varies as the parallelogram configuration varies; thus, with respect to the angular opening ϑ_1 and with respect to the distance between the phalanxes.

The mass m is the same for the different objects considered, while the shapes and sizes vary.

A metal-to-metal contact between gripper and object was considered in all simulations, which corresponds to a friction coefficient μ of 0.25.

7.1 Secure grip – Cylinders

The first simulations are based on the secure gripping of an object with the inner surface of the gripper (encompassing grasp region).

The object chosen for this evaluation is a $35\ gr$ mass cylinder in carbon steel (Carbon steel 1023, sheet metal (SS)) whose radius was varied to perform different simulations.

Its dimensions are initially $12mm \cdot 40mm$, so a radius of 6 mm was considered.

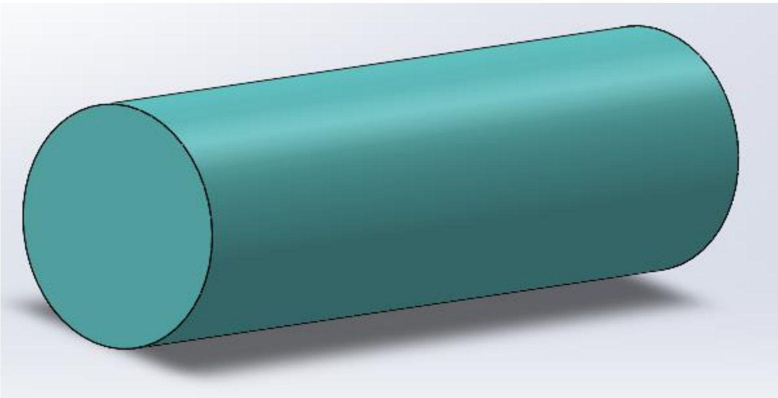

Figure 47: Cylindrical object

Then, in 'Motion Analysis' we add all the necessary contacts, add gravity that has an incoming direction to the simulation plane and finally a torsion of value $150\ N \cdot mm$.

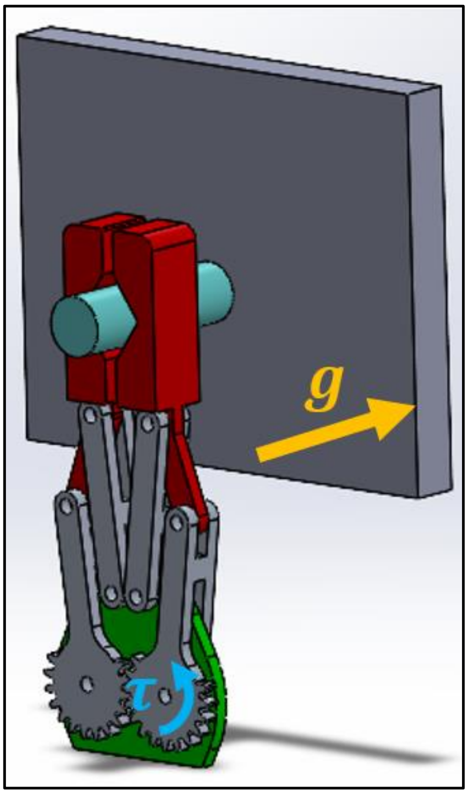

Figure 48: Setup configuration

Below is the figure representing the contact settings in SolidWorks:

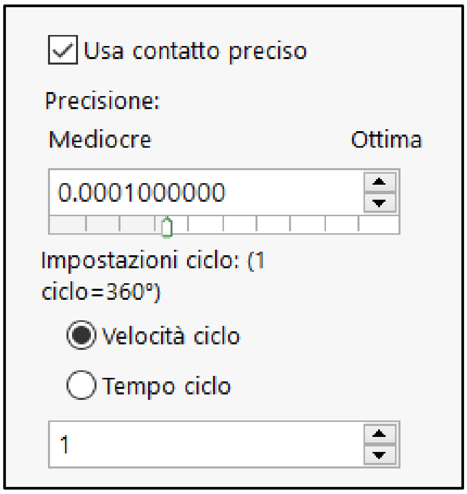

Figure 49: Contact settings

The following graph shows the contact force with the innermost fingertips of the gripper. As soon as contact is made with the object, there is a positive (left side) or negative (right side) peak. After contact has been made, the values settle at just over $2N$.

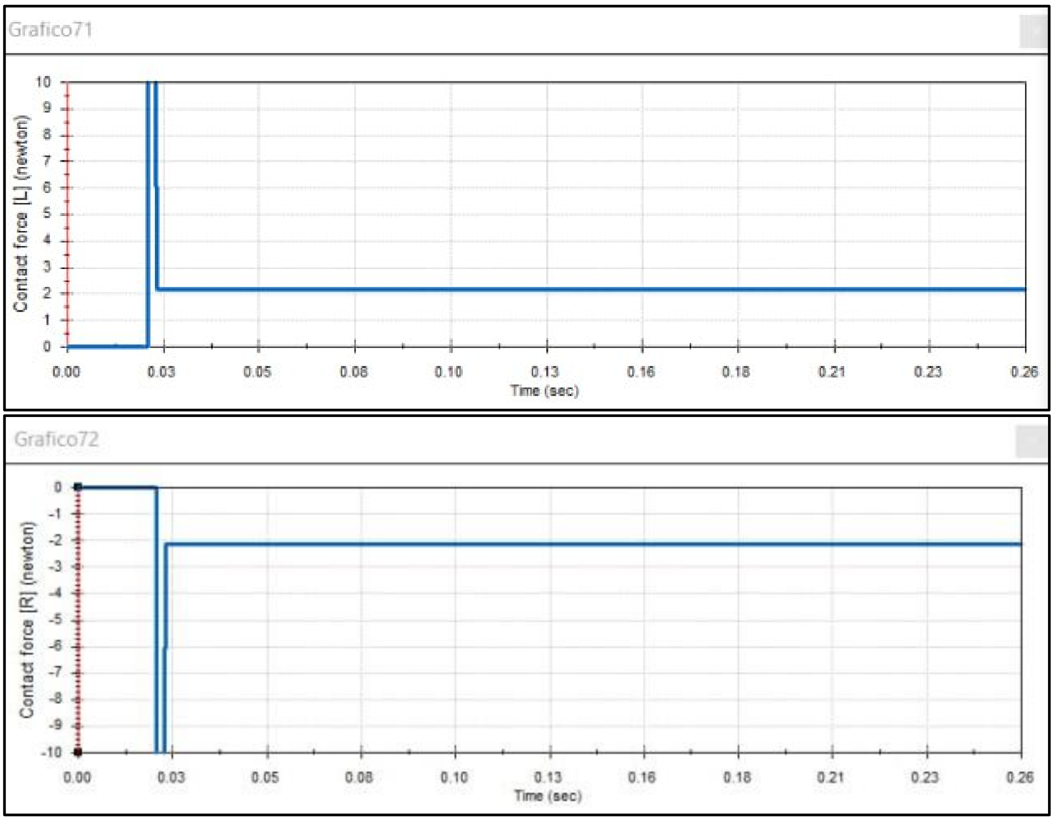

Figure 50: Contact force with the innermost fingertips

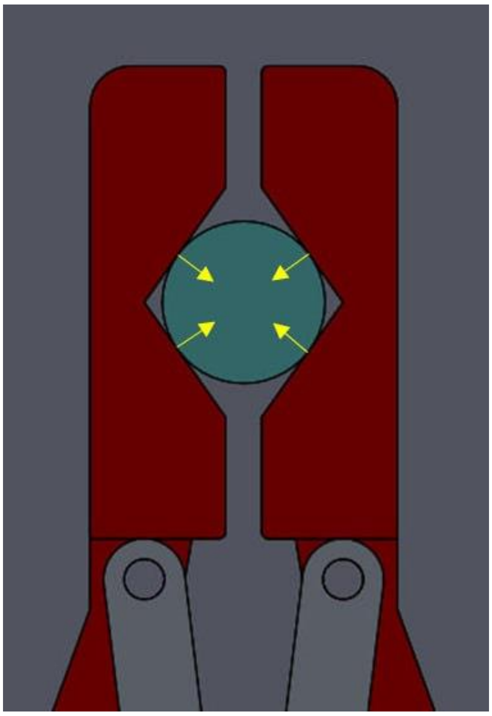

Figure 51: Vector forces – Secure grip

The perfect symmetry of the contact force values is visible. The gripper effectively holds the object without it slipping or falling on the plane.

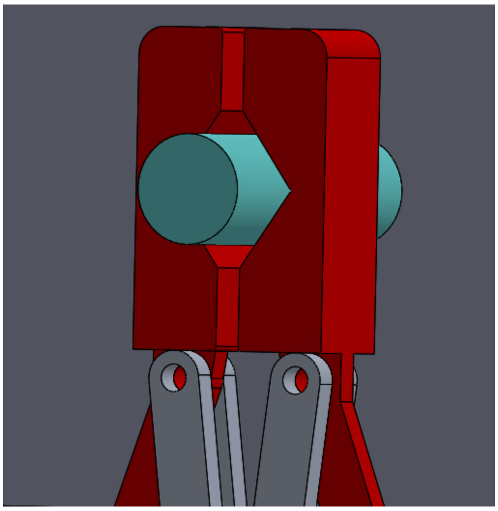

Figure 52: Secure grip - cylinder radius $6\ mm$

The same procedure was carried out for the other cylinders of different sizes.

- Cylinder size $20mm \cdot 40mm$, so a radius of $10\ mm$ was considered.

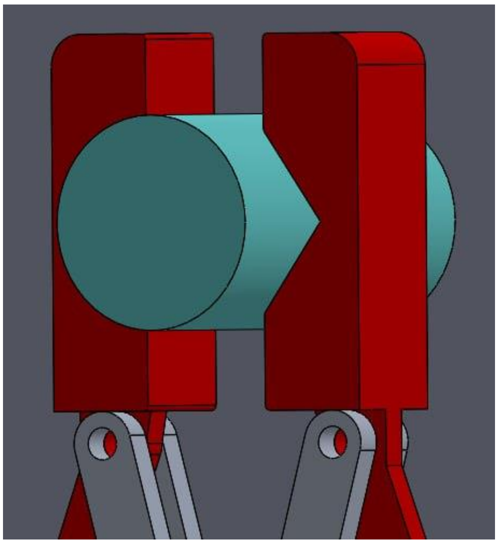

Figure 53: Secure grip - cylinder radius $10\ mm$

- Cylinder size $28mm \cdot 40mm$, so a radius of $14\ mm$ was considered.

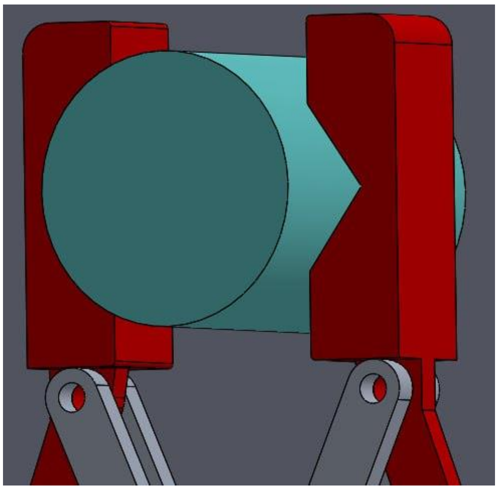

Figure 54: Secure grip - cylinder radius $14\ mm$

- Cylinder size $36mm \cdot 40mm$, so a radius of $18\ mm$ was considered.

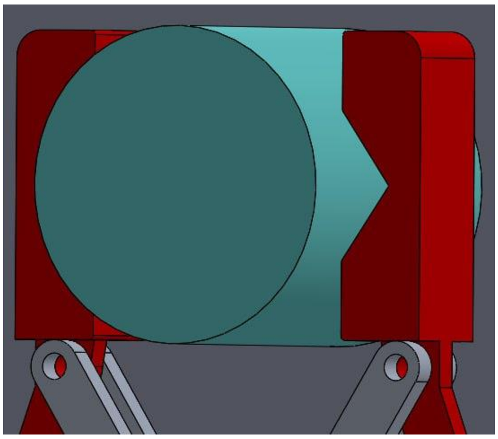

Figure 55: Secure grip - cylinder radius $18\ mm$

From the various simulations performed, the contact forces, the opening angle ϑ_1 and the corresponding distance between the gripper phalanges were extrapolated.

Using MATLAB, graphs relating these quantities were generated.

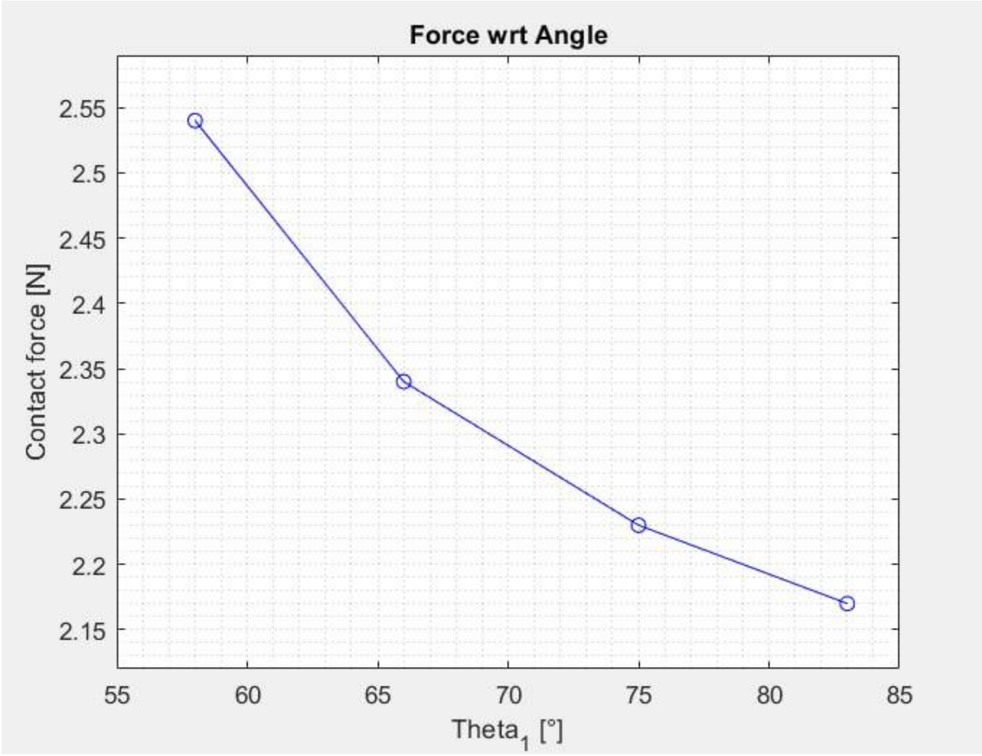

Figure 56: Force trend wrt angle

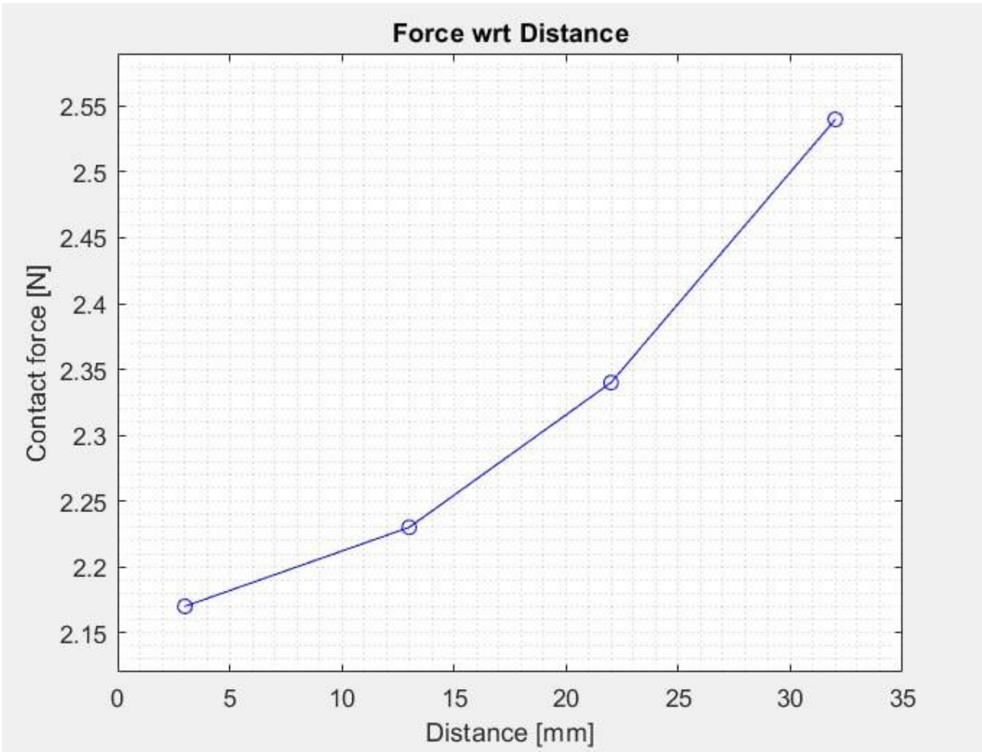

Figure 57: Force trend wrt distance

As the angle ϑ_1 decreases (i.e. as the distance between the phalanxes increases), with constant torque, the contact force between gripper and object tends to increase, even if minimally.

7.2 Precise grip - Rectangular prisms

These simulations are based on gripping the object securely, thus using the gripper's outer fingertips.

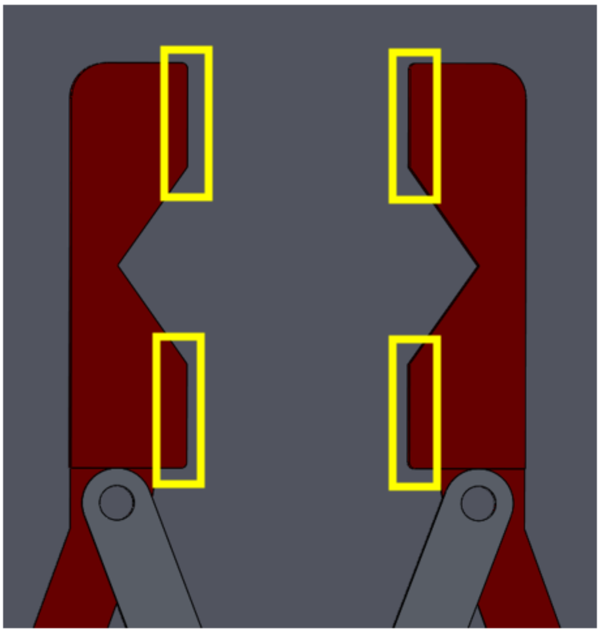

Figure 58: gripper's outer fingertips

Again, the object chosen for this evaluation is a 35 gr mass rectangular prism in carbon steel (Carbon steel 1023, sheet metal (SS)).

Its dimensions are initially $10mm \cdot 35mm \cdot 40mm$. The surface of the object resting on the plane measures $10mm \cdot 35mm$, so what varies is the first value, which indicates the distance between the phalanxes.

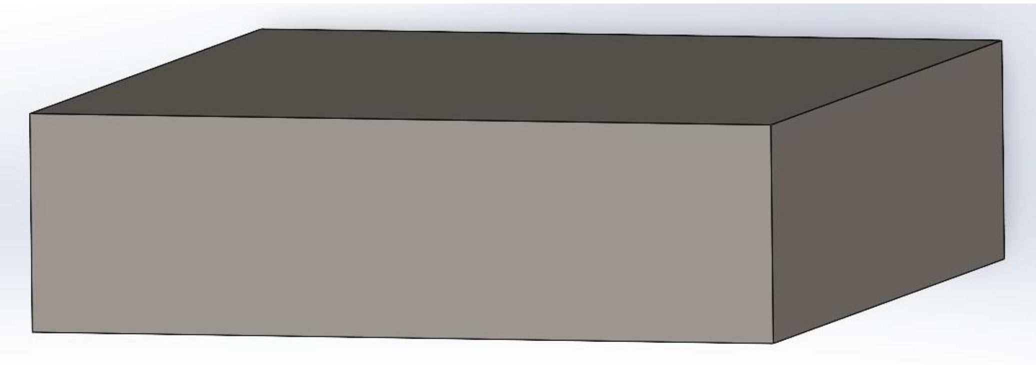

Figure 59: Rectangular prism object

The simulations carried out are set up in the same way as in the case of safe gripping of the cylindrical object:

- constant torque for all simulations of 150 $N \cdot mm$,

- gravity in the direction perpendicular to the plane.

As in the case of the cylinder, the values are also mostly symmetrical between the right and left side.

Thus, the contact forces are:

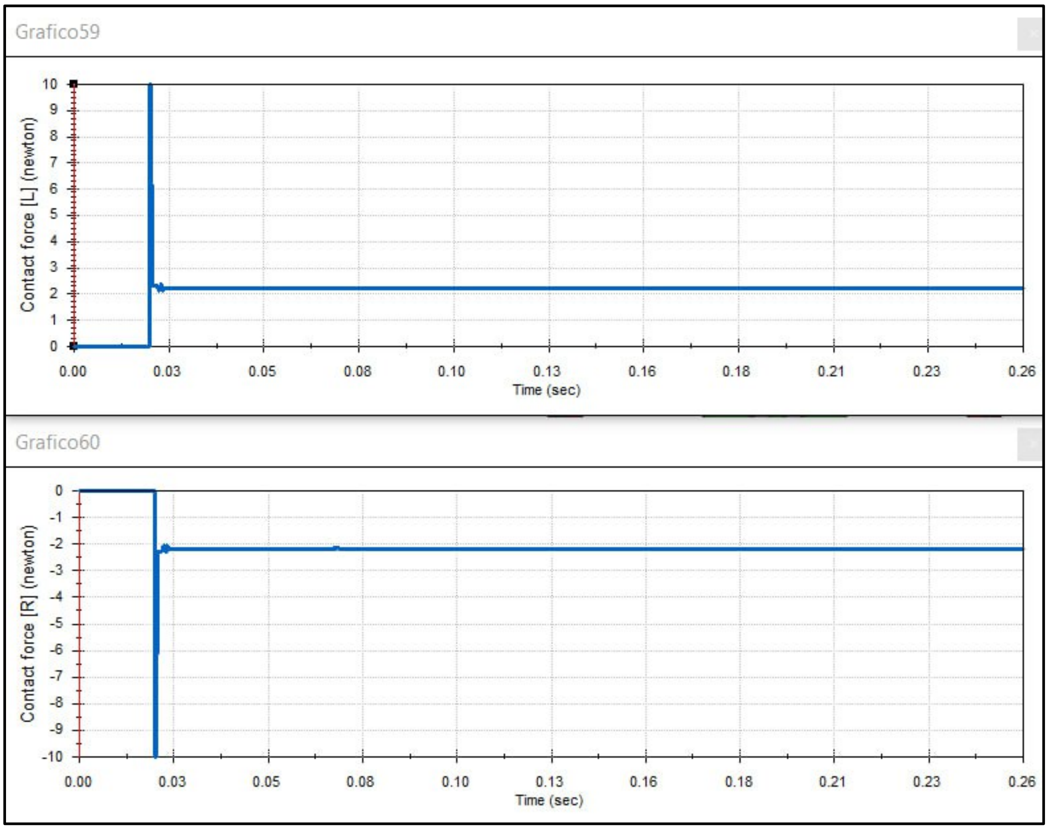

Figure 60: Contact force with the outer fingertips

The evaluated contact forces are depicted in the figure below:

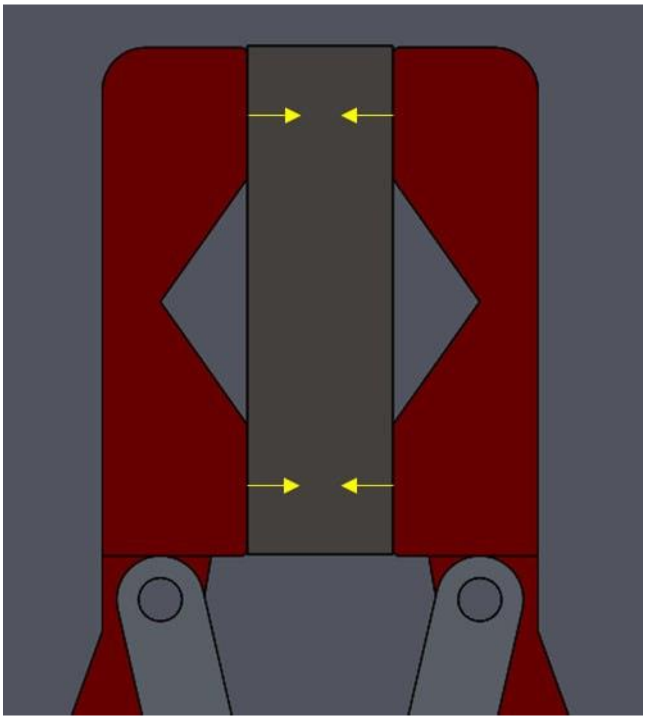

Figure 61: Vector forces – Precise grip

The same procedure was carried out for the other rectangular prisms of different sizes.

- Prism size $25mm \cdot 35mm \cdot 40mm$, so a distance between the phalanxes of $25\ mm$ was considered.

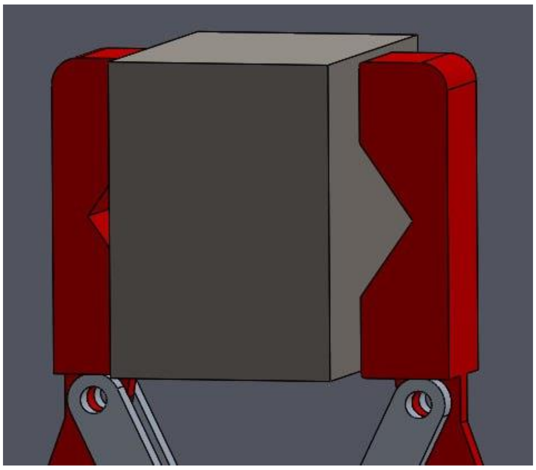

Figure 62: Precise grip - prism length 25 mm

- Prism size $45mm \cdot 35mm \cdot 40mm$, so a distance between the phalanxes of $45\ mm$ was considered.

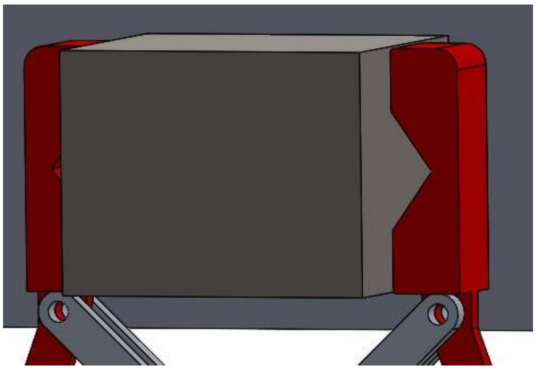

Figure 63: Precise grip - prism length $45\ mm$

- Prism size $60mm \cdot 35mm \cdot 40mm$, so a distance between the phalanxes of $60\ mm$ was considered.

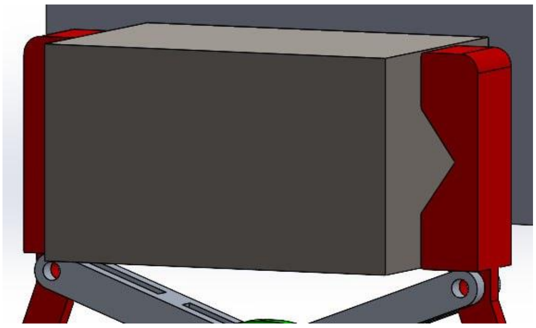

Figure 64: Precise grip - prism length $60\ mm$

From the various simulations performed, the contact forces, the opening angle ϑ_1 and the corresponding distance between the gripper phalanges were extrapolated. Using MATLAB, graphs relating these quantities were generated.

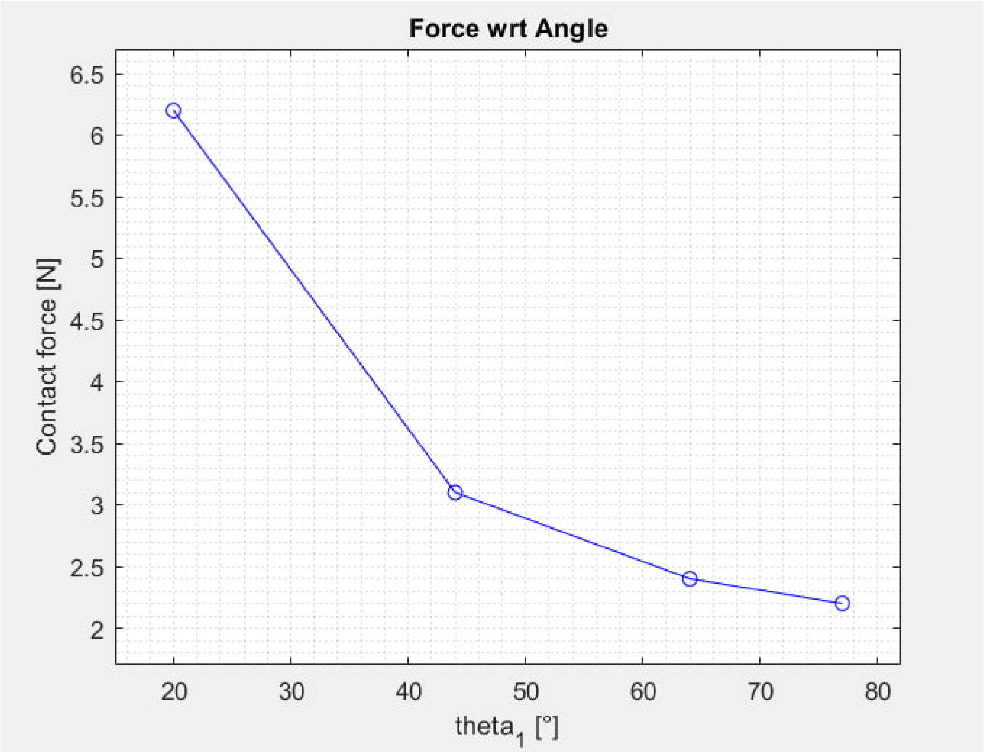

Figure 65: Force trend wrt angle

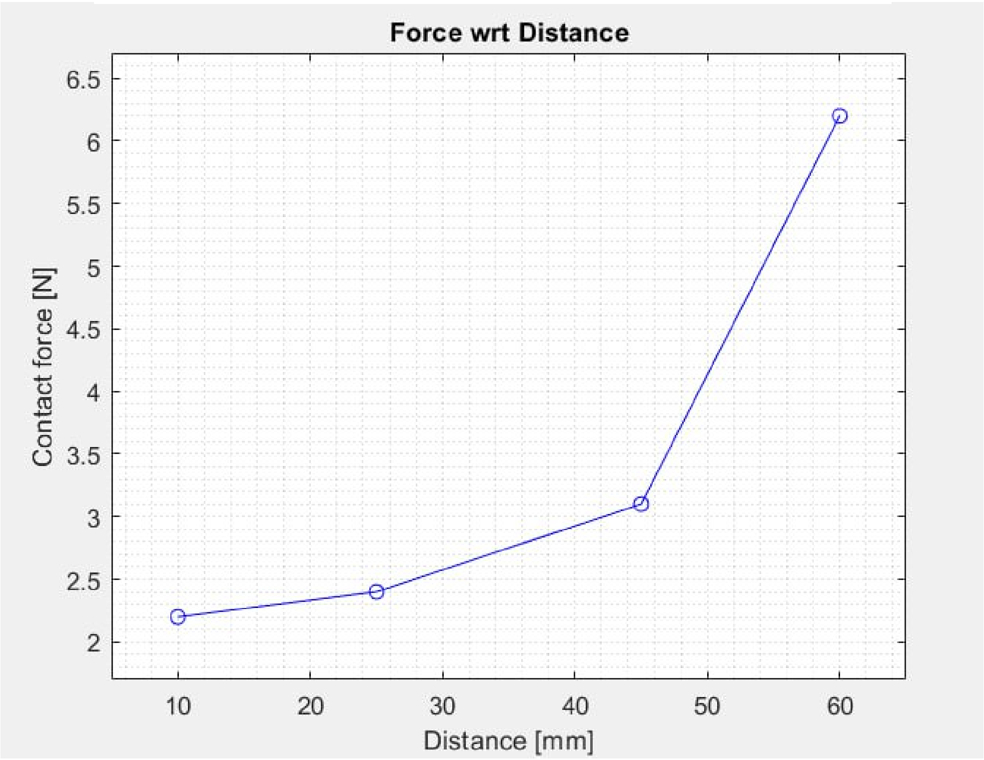

Figure 66: Force trend wrt distance

From the following MATLAB plots, the same behaviour obtained in the previous simulations is confirmed. As the gripper opening increases, the contact forces between object and fingertips tend to increase.

8. Conclusions

The robotic gripper project with parallelogram mechanism provided a significant opportunity to explore and explore various aspects of mechanical design and applied robotics. Through the various stages of the project, important considerations emerged that deserve to be emphasised.

Firstly, the kinematic analysis of the parallelogram mechanism demonstrated its effectiveness in maintaining constant object orientation during gripping operations. This aspect proved crucial in ensuring stable and precise handling, which is essential in many industrial and automation applications. The methodology adopted allowed the trajectories of the gripper points to be plotted, providing a solid theoretical basis for the subsequent design and simulation phases.

The component design phase on SolidWorks allowed the theoretical analyses to be translated into detailed three-dimensional models. This step was crucial to verify the feasibility of the design and to optimise the geometries of the different gripper parts.

Gripper simulations performed on various objects provided valuable information on the behaviour of the gripper under realistic operating conditions. These simulations revealed the gripper's ability to adapt to objects of different shapes and sizes, highlighting the versatility and robustness of the parallelogram mechanism. In addition, they made it possible to identify and solve possible gripping and stability problems, helping to refine the final design.

In conclusion, the project demonstrated how careful kinematic analysis, combined with detailed design and rigorous simulations, can lead to the development of an efficient and versatile robotic gripper. The skills obtained during this work will be of great value for future applications and projects in the field of robotics and automation.

Bibliography

[1] G.J. Monkman, S. Hesse, R. Steinmann, H. Schunk. “*Robot Grippers*”. Wiley, 2007.

[2] Anna Maria Gil Fuster. “*Gripper design and development for a modular robot*”. University of Denmark, 2015.

[3] Khurshid A., Ghafoor Abdul, Malik Afzaal. “*Robotic Grasping and Fine Manipulation Using Soft Fingertip*”. DOI-10.5772/23697

[4] Alif Aiman bin Ahmed. “*Type of gripper and gripper method*”. 2011.

[5] AURA Robotics, Adrian de la Iglesias. “*Brazo robotico y micro gripper*”. AIV, 2013.

[6] Elesa. “Organi di trasmissione”. https://www.elesa.com/it/CatalogoDatiTecniciIT/21-il-dente

[7] ROBOTIQ. “*Robotiq 2F-85 & 2F-140 for e-Series Universal Robots*”. Robotics Inc., 2018

[8] File Excel. Andamento degli angoli. Dati ricavati da SolidWorks.